



SAN FRANCISCO, CALIFORNIA

AUGUST 1-3, 1961

SHERATON-PALACE HOTEL

**SELF-CONTAINED SYSTEM
FOR
INTERPLANETARY NAVIGATION**

by

**R. L. Lillestrand
J. E. Carroll**

**Research Division
CONTROL DATA CORPORATION
Minneapolis, Minnesota**

PREPRINT 61-95

SELF-CONTAINED SYSTEM
for
INTERPLANETARY NAVIGATION

by
R. L. Lillestrand*
J. E. Carroll*

ABSTRACT

If the spin axis of an interplanetary vehicle is aligned normal to the ecliptic to within a few degrees, a rigidly mounted wide angle camera employing slits in its focal plane can provide all the necessary information for midcourse navigation. After the initial alignment of the spin axis no attitude controls are needed. By measuring the scan times associated with four stars, the orientation and dynamical motion of the slowly spinning vehicle can be calculated; by measuring the scan times for two planets, the position of the space vehicle can be calculated by triangulation.

While no moving parts are required if the vehicle is spin stabilized, the detector requires only one rotational degree of freedom if the vehicle is inertially stabilized. With this single axis of rotation all three attitude axes can be determined as well as planetary sight lines for triangulation. Accuracies of the order of 10 seconds of arc are achievable.

In the case of the planets, the observing instrument with its scanning slits measures the position of the planetary limb only. Thus problems associated with variable solar aspect angle, a poorly defined planetary terminator or variations of the albedo across the illuminated planetary surface are avoided. Navigational data can be provided over a large fraction of an interplanetary or lunar mission since the system can operate to within about one planetary diameter of the Earth or the terminal planet.

* Research Division, Control Data Corporation, 5710 West 36th Street, Minneapolis 16, Minnesota.

SELF-CONTAINED SYSTEM FOR MID-COURSE NAVIGATION

INTRODUCTION

The accuracies needed for an interplanetary mission are such as to require that the space vehicle's mid-course position be accurately known in order to introduce corrective thrusts. A precise method is therefore needed for the navigation of the vehicle. While a variety of Earth-based schemes using radio techniques have been suggested in the past, the present paper considers a self-contained optical navigation instrument which is particularly attractive because of its extreme simplicity and accuracy.

Brief Description

While the simplest configuration using the detection instrument described in the present paper is that in which it is body-mounted on a spin stabilized vehicle, it is also possible to use this instrument on an inertially stabilized vehicle by allowing it to spin about an axis normal to the ecliptic. The viewing instrument is a wide angle camera equipped with slits in the focal plane and thus a region on either side of the ecliptic plane is scanned. The viewing geometry is shown in Figure 1.

When the energy from a star or a planet falls on one of the slits a photo-multiplier detects this radiation, and by measuring the time of these pulses the position of the celestial body can be determined. This requires that we obtain at least two slit scan time measurements. For the slit arrangement shown in Figure 2A the sum of these two time measurements defines the azimuth position of the target while the difference of these two time measurements defines the elevation position. The positions of the planets are derived from a measurement of the position of the illuminated planetary limb. Since the approximate position of the space vehicle is known, a correction for the separation between the planetary limb and the center of the planet can easily be introduced. Should the scanning direction be such that the terminator is approached first rather than the illuminated limb, the times of decay will be measured rather than the rise time as is shown in Figure 2B.

The basic postulate of this system which measures time rather than angle is that the motion of a spinning space vehicle behaves dynamically like a rigid body spinning in a field free of externally imposed torques. Typically spin periods of 10 to 100 seconds/rotation are used, although its rate is not critical and need not be known beforehand. The direction of the spin axis need be normal to the ecliptic to an accuracy of only a few degrees. As a result, attitude control equipment can remain

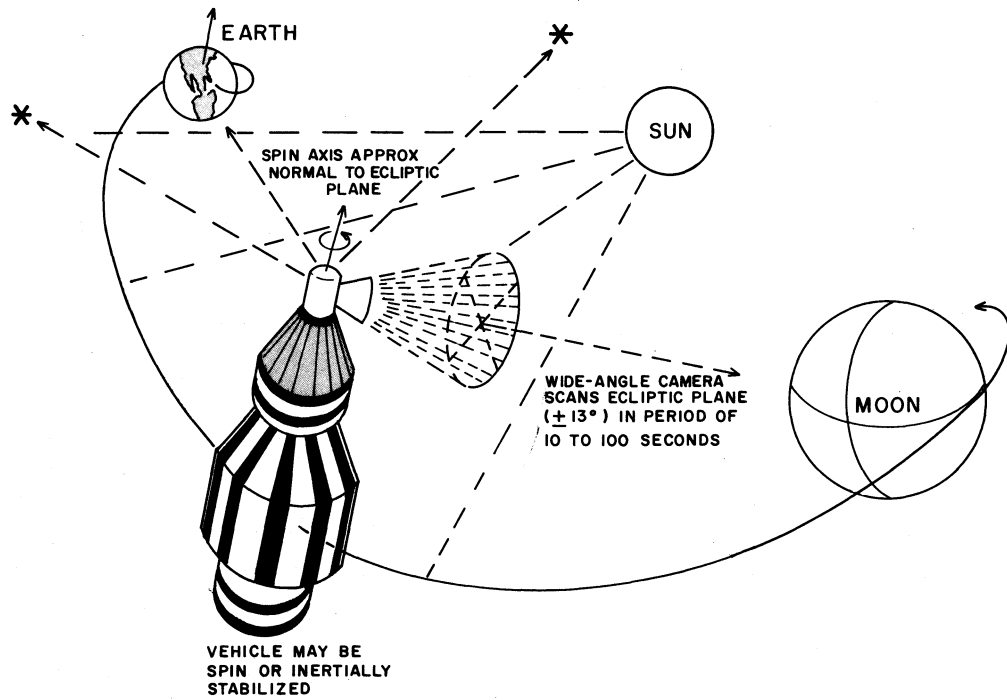


Figure 1. Geometry of Mid-Course Navigation

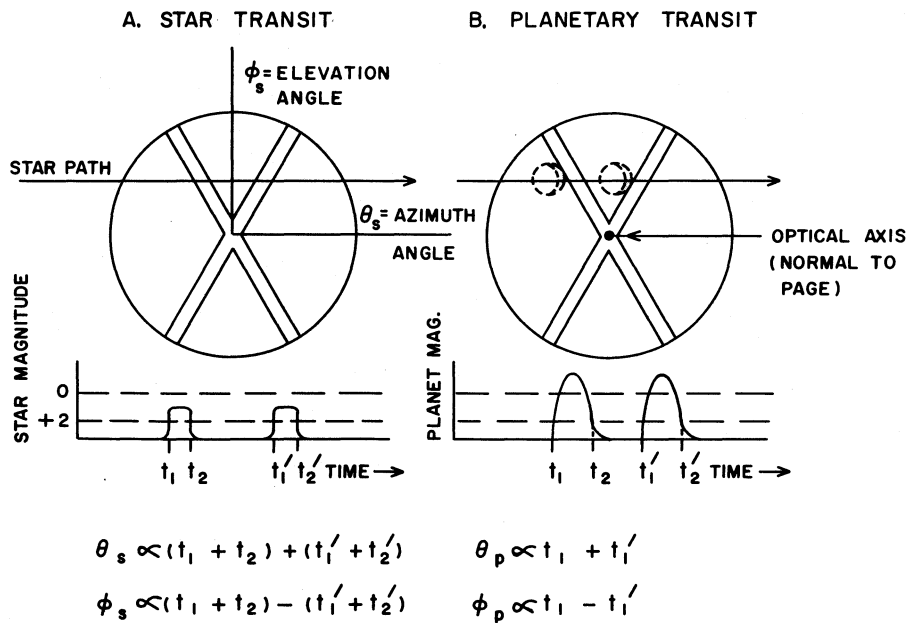


Figure 2. Use of Slits at Focal Surface of Rotating Camera to Determine Target Position

quiescent over prolonged periods and useful navigational information can be collected with no mechanisms for precision pointing of the camera or the spin axis. The fact that angle measurements are not made directly but only through the intermediary of time measurements is particularly advantageous since time measurements can be made to an accuracy of one part in 10^6 relatively easily, however angle measurements to this accuracy are extremely difficult and often require complex instrumentation.

Comparison With Other Instruments

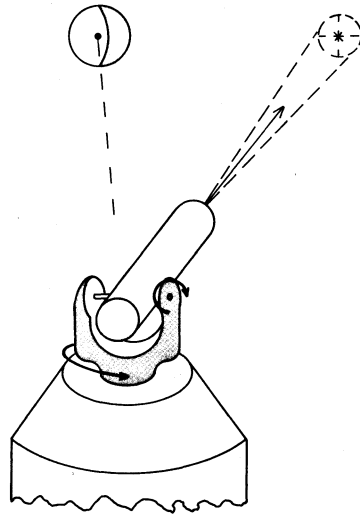
In the past, several types of optical instruments have been proposed for mid-course navigation. However, most of these instruments require the use of gimballed optical trackers or cameras for determining the positions of the various planets and they therefore lead to relatively complex instrumentation. Three optical devices which might be applied to the mid-course navigation problem and which are shown in Figure 3 are:

- 1) Absolute measurement of angles between planets with gimballed star tracker mounted on inertially stabilized platform.
- 2) Relative measurement of position of planets and surrounding star field with wide-angle camera equipped with image tube.
- 3) Measurement of transit time for stars and planets with rotating wide-angle camera equipped with slits in focal plane.

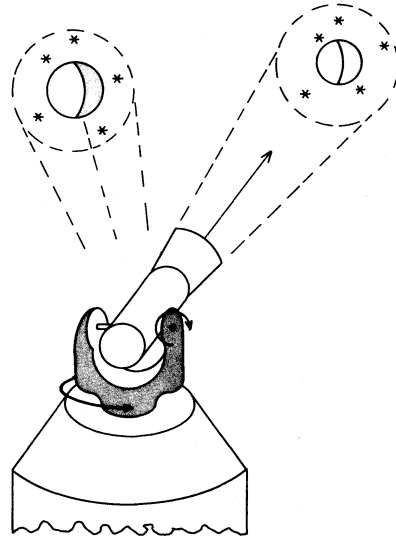
Larmore¹ has discussed a variety of techniques for the determination of the orientation and position of a space vehicle which rely on the measurement of angles between various planetary and stellar targets. In this case, a gimballed optical tracker is assumed to be available which is accurate to approximately 0.2 second of arc. Aside from the difficulty of constructing the tracker's angle encoder to this accuracy, this instrument presents difficult design problems in terms of the target acquisition, in terms of locating the center of gravity of the planets, and in terms of the considerable weight and complexity of an automatic tracking theodolite. Similar difficulties would be encountered with the optical tracker mounted on an inertial platform as proposed by Bement.²

The second type of system mentioned above which measures the position of the planetary target relative to the field of stars which surround it, circumvents the problem of accurate large-angle measurement. In this case the position of the planet relative to stars lying within a radius of a few degrees is determined. This system has the added advantage that the orientation of the platform to

A. AUTOMATIC TRACKING THEODOLITE
PROVIDING MEASUREMENT OF
ABSOLUTE ANGLES BETWEEN
WIDELY SEPARATED TARGETS



B. WIDE-ANGLE TELESCOPE FOR
MEASUREMENT OF PLANETARY
POSITION RELATIVE TO
NEARBY STARS



C. WIDE-ANGLE SCANNING CAMERA
USING SLIT TRANSIT TIME
MEASUREMENTS

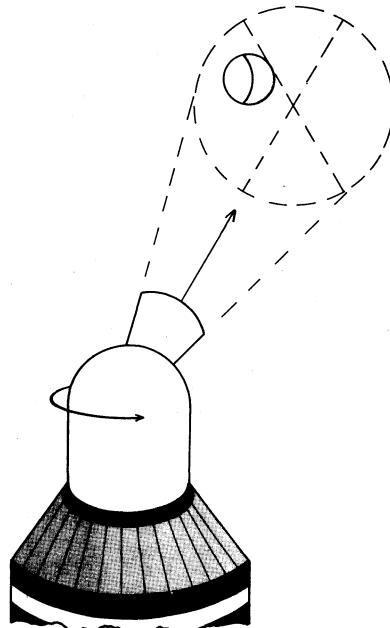


Figure 3. Types of Optical Instruments for Mid-Course Navigation

which the wide-angle camera is attached need not be known, or held constant. However, with this system one must either employ two wide-angle cameras to concurrently track two objects within our solar system, or one must be prepared to point the camera back and forth from one target to the next. Thus this technique may require auxiliary equipment for target acquisition. In addition, this approach has the disadvantage of requiring the use of relatively faint stars--between 8th and 10th magnitude. Thus the star identification problem becomes difficult. If one attempts to minimize this problem by enlarging the field of view of the camera to find brighter stars, a loss of accuracy results. Typically the resolution of an image tube ranges from 300 to 1000 lines and therefore to obtain an accuracy of 5 seconds of arc, one cannot use a field of view greater than about 2 degrees. Examples of this type of system are those described by Bock³, Cardozo⁴, and de Kler.⁵

The instrument which employs a wide-angle camera with a system of slits in the focal plane and a photomultiplier as a detector (Number 3) is the one which will be described in the present paper. In terms of both mechanical and electrical complexity, it represents an improvement over the other two detection instruments. In terms of accuracy potential, it is at least comparable. Depending on the specific design and use of the detection instrument, an accuracy ranging from 1 second of arc to about 1 minute of arc may be expected.

Probably the most important advantages of the instrument described in the present paper are: (1) that it involves few or no moving parts, (2) that it uses stars brighter than 2nd magnitude, (3) that time is measured rather than angle, and (4) that the problem of finding the center of the planets is solved by measuring the position of the illuminated planetary limb. Certain additional advantages can be gained in terms of the reduction of the position error sensitivity coefficients because the positions of all of the solar system bodies brighter than some predetermined magnitude are measured during each 360° rotation of the camera. This is described in the section: Statistical Determination of Position.

An instrument similar to that discussed in the present paper is described by Willmore⁶ for tracking satellites from a ground-based station. This instrument achieved an accuracy ranging from 15-60 seconds of arc with a telescope of 5 inch aperture and 14 inch focal length, however it had a very much smaller field of view. A further description of Willmore's instrument was made by Groves and Davies⁷ in their paper on methods of analyzing observations of satellite orbits.

Position Fixing

Two basic methods of position fixing can be used and these are shown in Figure 4. The first method is that of the measurement of the relative angles between three planets. This method does not require any star position measurements to determine the position of the space vehicle. It is commonly used in surveying and photogrammetric work. Papers by Carroll⁸, Atkinson⁹ and Stearns and Frye¹⁰ describe this technique. The Three-Planet Method is subject to large errors when the position of the space vehicle lies on the circle defined by the three known planets.⁸ A study of various space vehicle viewing geometries indicates that one of the three planets is often at a considerably larger distance than the other two and thus it contributes disproportionately to the position error. Also it was found that when the three planets fall within an azimuth angle significantly less than 90° (as is shown by the case of the dotted lines in Figure 4A), the error sensitivity coefficient for the position of the space vehicle normal to the ecliptic plane becomes large.

A method which appears to yield smaller error sensitivity coefficients over a wider range of interplanetary vehicular positions is shown in Figure 4B. This method is that of simple triangulation using two known solar-system bodies, and as such it can be used for a lunar mission while the

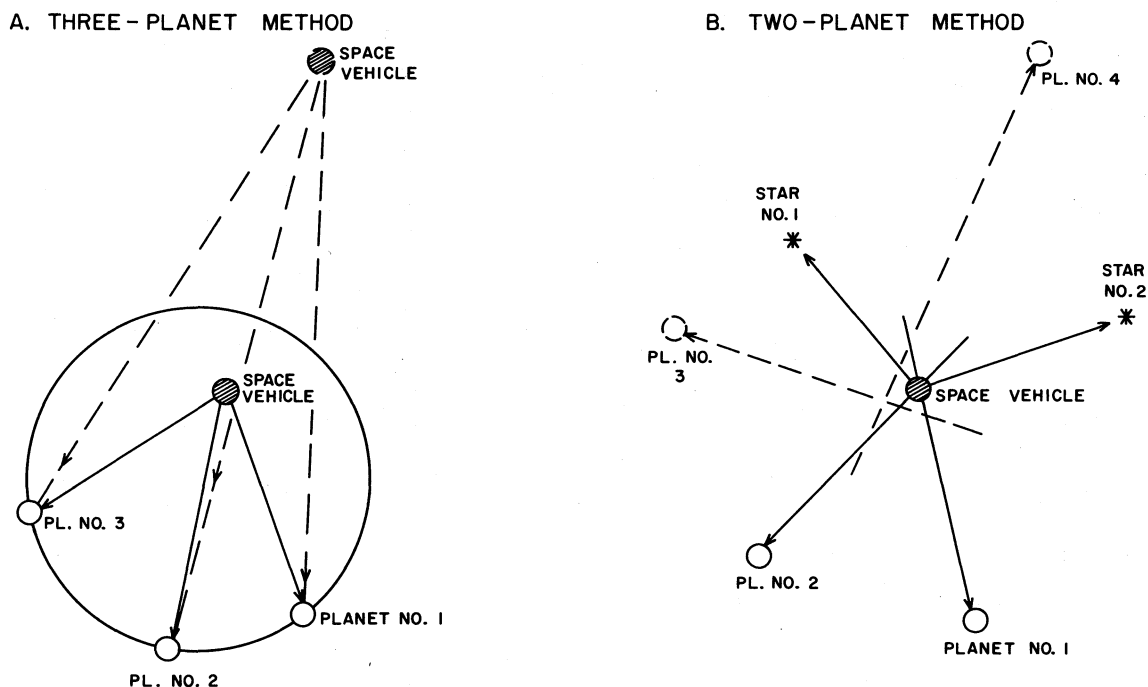


Figure 4. Methods of Position Fixing

Three-Planet Method cannot. In this case information obtained from the star transits is used to provide a spatial attitude reference. A non-redundant position fix is obtained from the two angular coordinates of one planet (thus establishing the direction of a line in space) and one angular coordinate of the second planet. This coordinate will be the azimuth angle, i. e., the angular bearing of the planet measured in the ecliptic plane. The error sensitivity for the triangulation will be minimized by selecting the shortest sight lines which are most nearly orthogonal, thus it is evident that the Earth and the terminal planet will not always be the best selection for triangulation during an interplanetary mission.

Since our detection instrument provides angular position data from at least 6 solar-system bodies, the question presents itself as to how one selects the best pair of bodies for the position fix. In fact, at any one time certain space vehicle position errors might be minimized by one pair of bodies while other position coordinate errors are minimized with other planetary pairs. For the Earth-Mars flight described in the Applications section, it happens that these two planets form the best basis for position calculation over most of the transfer orbit. However, since conditions will vary widely for various transfer orbits, the Two-Planet Method requires a careful study of position error sensitivity coefficients if the greatest accuracy is to be achieved. In this respect, it is no better than the Three-Planet Method.

In order to resolve this problem and to take full advantage of all observational data on solar-system bodies, a statistical technique has been developed which is based on least squares polyangulation. This technique regards each body as defining a line in space whose positional uncertainty may be considered to be proportional to the product of the length of the line and the estimated rms angular error in the measurement of the position of the body. The dotted lines in Figure 4B show this geometry with two additional planets. In this case the weighted least square position of the space vehicle is determined without ever performing a simple two-planet triangulation. The polyangulation automatically weights most heavily those sight lines which carry the least positional uncertainty. Thus, as a space vehicle travels from Earth to Mars it might happen that the position fix is dominated by data from the Earth and the Moon early in the flight; at mid-course the Earth and Mars sight lines might have the heaviest weight; at the terminal phase, Mars and its Moons, Phobos and Deimos, will dominate the position calculation.

MOUNTING OF DETECTION INSTRUMENT

The basic requirement in mounting the wide-angle camera to the space vehicle is that it must be provided with a spin motion in inertial space in order to scan the region of the sky near the ecliptic. If the vehicle itself is spin stabilized, the wide-angle camera can be rigidly attached to the vehicle so that the detection instrument requires no moving parts. On the other hand, if the vehicle is stabilized in inertial space, the camera must be provided with a degree of rotational freedom relative to the vehicle.

Inertially Stabilized Vehicle

In this case one degree of rotational freedom is sufficient to provide data for the calculation of all three attitude axes plus the three coordinates of position. As is shown in Table I there are two basic methods which can be used to measure the angular position of the rotating camera at the time of transit of a celestial body.

TABLE I: METHODS OF MEASURING POSITION OF PLANET TRACKER WHEN USING INERTIALLY STABILIZED VEHICLE

Basis of Measurement	Instrumentation Required (In Addition to Camera and Detector)	Description of Method	Advantages of Method
1. Time Difference	Clock	Assuming the camera is spinning at constant angular velocity, the time of transit of various celestial targets is measured.	<ol style="list-style-type: none"> 1. Does not require accurate space vehicle inertial stabilization. 2. Instrumentation for clock is simpler than that of angle encoder. 3. Clock is more accurate than angle encoder.
2. Relative Angle	Angle Encoder	Assuming the space vehicle remains motionless in inertial space, the angle of the camera relative to the vehicle is measured at the time of appearance of the various celestial targets.	<ol style="list-style-type: none"> 1. Does not require camera spin rate to be constant relative to inertial space.

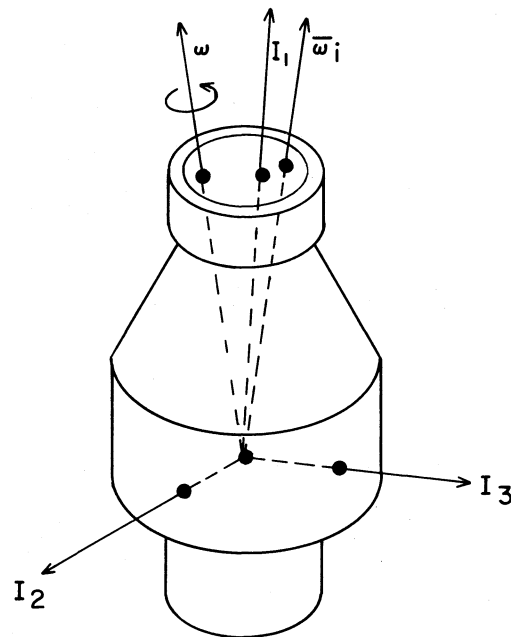
The first method which involves the measurement of time is predicated on a constant spin angular velocity. Any variations in camera spin rate in inertial space will impose a limit to the accuracy of this method. On the other hand, variations in the rotation of the vehicle itself about the camera spin axis will cause no error. Should the vehicle have residual rotational components about either of the other two axes because of gyro drift, these potential sources of error can be eliminated by collecting data during several rotational cycles. Using a spin period of 10 seconds, a clock which is stable to one part in 10^6 (or 10 microseconds) will give an equivalent angle accuracy of 1 second of arc. Since clocks of this accuracy are available in relatively simple form, while angle encoders to this accuracy seem to involve complex electronics or large and heavy transducers, it is evident that the first method is potentially the most accurate. However, the problem of slowly rotating the camera at a uniform rate presents an extremely difficult design problem and a hybrid encoder using periodic angle check points with linear time interpolation is recommended. An increase in the spin rate will relieve this problem, however this will eventually lead to a more difficult computer problem by requiring more elaborate statistical techniques and the sampling of data over many rotations of the camera.

Spin Stabilized Vehicle

If we assume that the vehicle is spin-stabilized about an axis which is within $\pm 5^\circ$ of the normal to the ecliptic, then a camera whose axis is more or less orthogonal to the spin axis will scan the region of the ecliptic. Depending on the dynamics of the spinning motion, as many as 4 stars and 2 planets may be needed for the complete determination of the space vehicle's attitude and position. If a nutation damper is used to prevent the vehicle from spinning about any axis but a principal axis of inertia, only two stars will be needed for the determination of the attitude of the vehicle. Several methods of damping nutational vibrations are described by Newkirk, Haseltine and Pratt.¹¹

The motion of a free spinning vehicle may be relatively complex and Figure 5 shows the principal factors which must be considered in analyzing the star transit time measurements of a spin stabilized vehicle. The simplest case will occur if the spin axis and the instrument axis are parallel with a principal axis of inertia. In this case there will be no force-free precession and only two stars are needed to completely describe the space vehicle attitude as a function of time. Actually

the structural deformations of the space vehicle will deflect the instrument axis* after the initial ground-based alignment, and one additional star is needed to define the magnitude and direction of this deflection. This star should be picked to be as nearly opposite one of the other stars as is possible in order to accurately calculate the deflection. If the principal moments of inertia are not equal and if the spin axis does not coincide with a principal moment of inertia a force-free precession will result.¹² The spin axis will move in a conical path relative to the space vehicle and the space vehicle axis will move in another conical path relative to an inertial reference frame. The first path is known as the polhode and the second as the herpolhode. The result of these motions is to force us to use more than 3 stars during a single rotation of the space vehicle or to make a second set of star transit measurements during a succeeding rotation.



I_1, I_2, I_3 = PRINCIPAL MOMENT OF INERTIA
 $\bar{\omega}_i$ = DIRECTION OF INSTRUMENT AXIS
 $\bar{\omega}_s$ = DIRECTION OF SPIN AXIS

Figure 5. Factors Effecting Star Transit Times in Spin Stabilized Vehicle

* The instrument axis lies in the plane normal to the optical axis of the camera and is parallel with the scanning slit elevation axis (Figure 2).

DESIGN OF DETECTION INSTRUMENT

The instrumentation required for the navigation system may be divided into three major parts: (1) the reference clock used to convert time measurements into equivalent angle measurements, (2) the digital computer required to convert the scan time data into space vehicle position data and (3) the wide-angle camera and its detection electronics. The present paper will concentrate on the design of the detection instrument and the way in which this design leads to a navigational capability. The reference clock is used to measure the time of occurrence of scanning pulses and will require an accuracy no greater than 10^6 . It therefore does not present any particular design problem.

The computer will be on-board, if a self-contained navigational capability is required as has been assumed for the present paper. Our present analysis indicates that the computer requirement can be easily fulfilled with the Control Data Corporation High Reliability Space Computer. This is a general purpose parallel computer designed to have a 95% probability of unattended operation for one year. This high level of reliability as compared with present computers is required for the extended periods of interplanetary missions. This design employs multiple-level redundancy techniques developed by Control Data Corporation. This computer occupies approximately 0.3 cubic foot, weighs 15 pounds, and requires some 20 watts of power. The memory contains both a magnetic core and magnetic drum section each of 4096 12-bit words and having access times of 6.4 microseconds and 10 milliseconds respectively.

Optical Design

The dominant factor affecting the optical design is the requirement of a relatively wide field of view, about 30° , in combination with a high image quality over the full field of view. Since we wish to measure the positions of the stars and planets to an accuracy lying between 10^{-4} and 10^{-5} radians, we require that the blur circle falls within this same range. A representative optical design which meets these requirements is shown in Figure 6. This design is the Baker-Nunn Satellite-Tracking Camera which was constructed during the International Geophysical year under the direction of the Smithsonian Astrophysical Observatory.¹³ The original camera had a field of view of 30° and

an aperture of 20 inches. The focal length was also 20 inches and the image diameter about 10 seconds of arc. In our case, we have assumed that this design is scaled down to a 4 inch aperture, and that the image diameter can be held to 10 seconds of arc. The characteristics of this optical design are shown in Table II.

TABLE II. CHARACTERISTICS OF REPRESENTATIVE OPTICAL SYSTEM

Type of Camera	Baker-Nunn
Aperture	4 Inches
Field of View	30 Degrees
f Number	1.0
Effective Focal Length	4.0 Inches
Diameter of Primary	5.5 Inches
Diameter of Focal Surface	2.0 Inches
Diameter of Blur Circle	10 Seconds of Arc
Focal Surface	Slits can be made to conform to whatever surface minimizes optical aberrations.
Spectral Region	4500 Å to 7000 Å
Distortion	If known, correction factor can be introduced.

One might think that the relatively short focal length, 4 inches, would present a limitation to accuracy, however it does not. The slits can be positioned on the more or less spherically curved focal surface to an accuracy of 10^{-4} inches. This is equivalent to an angle of $10^{-4}/4$ radians, or only 5 seconds of arc. As will become evident from the discussion which follows, the region between the slits is open and causes no blocking. One can expect a certain amount of distortion for images which are near the edge of the field, however the distortion is radial (that is, the images are displaced towards or away from the point where the axis intersects the focal surface) and therefore a correction factor can easily be included in the computation of the relative angles. Freedom from distortion requires that the tangent condition is satisfied ($x/\tan \theta = \text{constant}$) and freedom from coma requires that

the sine condition be satisfied ($x/\sin \theta = \text{constant}$), thus it is evident that the optical system cannot be free from both of these aberrations at the same time. However, since coma and most of the other aberrations of the optical system will be symmetric about a radial line, our system of radial slits will eliminate their effects. The major aberration of the optical design shown in Figure 6 is that of field curvature. However, by means of a system of slits curved to conform to the focal surface, this aberration causes no difficulty.

Slit and Detector Design

The scan time measurements are obtained by measuring the time at which the star image falls on the photomultiplier as the radiation reaches the edges of the slits. This was shown in a general way in Figure 2. Figure 6 shows the slit design when glass fibers are used to collect the radiation passing through the slits. After passing through one of the slits, the radiant energy of the star must be directed to the photocathode. One way of accomplishing this would be to shape the photosensitive surface to conform to the focal surface, but this is not desirable for several reasons. First, the size of the focal surface will be about 2 inches in diameter, and the photomultiplier dark current should be minimized by the use of the smallest diameter photocathode. A photocathode of more nearly 0.5 inch diameter is desirable. Second, we wish to spread the image out over a large portion of the photosensitive surface in order to average out microscopic regions of varying sensitivity to make an accurate intensity measurement. For this reason, the photocathode should be displaced from the focal surface. Since we are dealing with a very wide-angle cone of light, the displacement will not have to be very great in order to accomplish a significant dispersion of the radiation.

The method of collecting the energy which passes through the slits is that of a dielectric optical fiber. If a star image impinges on the end of one of the fibers, which are positioned at the focal surface, it will be transmitted along the transparent cylinder after a succession of multiple internal reflections. Provided the radius of the curvature of the bends is not too small, the light can then be piped to any place where it is convenient to mount the detector. In the case shown in Figure 6 the glass fibers are drawn out through the spiders which support the two crossed slits. They are then drawn to the face of the photomultiplier. In this case we have shown separate photomultipliers for each of the slits. Since each slit transmits light to a different photomultiplier the response must be normalized by using a calibrated light source. This light source also provides an absolute

reference for the preliminary identification of stars and planets by means of an intensity measurement. The double photomultiplier arrangement is used because it makes it possible to measure the planetary limb when the planet subtends an angle as large as 50°. Thus, the camera can not only provide information for midcourse navigation, but it can also provide useful information during the early and terminal phases of the mission.

The photomultipliers must be protected from the Sun and therefore a shutter is needed between the ends of the glass fibers and the photocathode. If a silicon solar cell is mounted on both sides of each of the slits, the power for the actuation of the shutter can be derived from the Sun itself. Since the Sun is about 30 minutes of arc in diameter and the slits only 1 minute of arc, there will be a continuous signal available for all positions of the solar image when it is in the neighborhood of the slit. If the outside edges of the silicon solar cells are accurately located, the time of build-up of this signal can be recorded and the relative angular position of the Sun can be determined.

The width of the strip across the celestial sphere which is scanned by the camera will be less than the field of view of the camera. This comes about because of the necessity of deriving elevation as well as azimuth position information as is shown in Figure 6. The use of orthogonal slits would give equally accurate azimuth and elevation position measurements; however, the width of the scanned field is only 21.2°. With a slight degradation in elevation accuracy, this field can be increased to 26° by cutting down the angle between the slits to 60°. A variety of other slit configurations have been considered, but all fundamentally yield the same result illustrated by the simple crossed arrangement of Figures 2 and 6.

Because of the rotation of the detection instrument, the motion of a star or planet along the focal surface of the optical system will resemble a line of constant latitude on the earth. Thus, if the slits were great circle arcs on a spherical focal surface, the relation between the difference in the time a given star crosses the slits and the elevation angle is not proportional. If ϕ is the elevation angle of the star relative to the optical axis, if Δt is the difference in slit scan times, and if T is the rotational period of the camera, then

$$\phi = \tan^{-1} \left[\frac{\sin \left(\pi \frac{\Delta t}{T} \right)}{\tan \eta} \right] \quad (1)$$

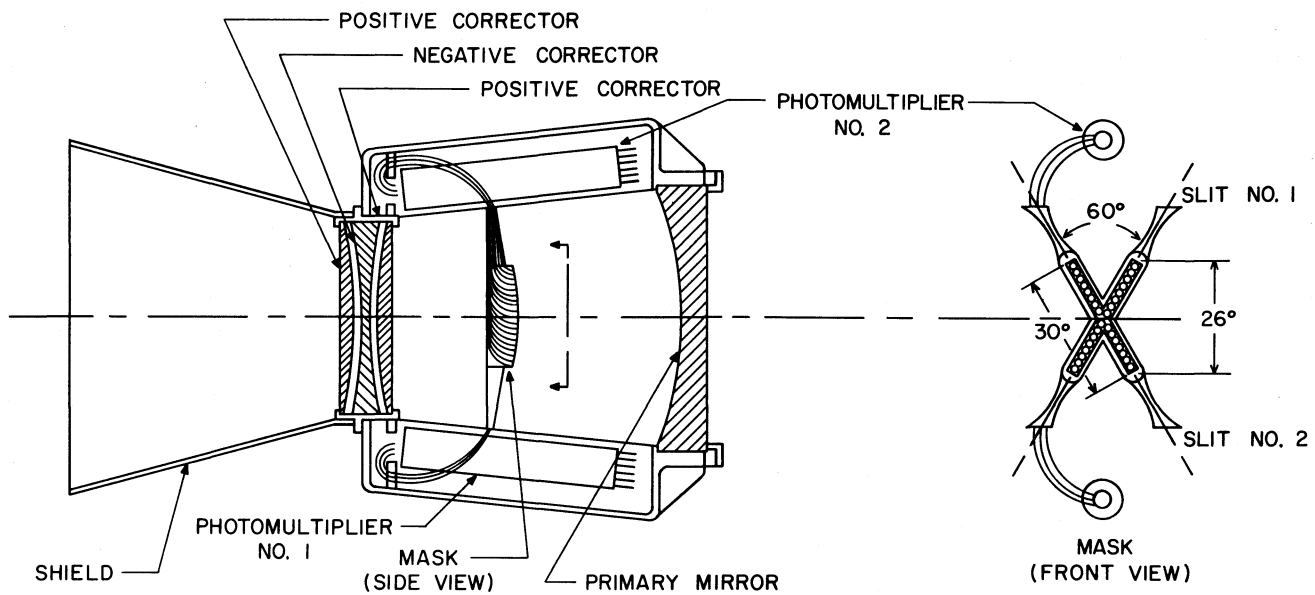


Figure 6. Representative Wide-Angle Camera

Statistical Limits

Theoretically a telescope which continuously points toward a star over an extended interval of time can locate its position much more precisely than can a scanning camera which views the star intermittently for short intervals of time. For example, if one regards the arrival of incoming photons as random events which have a spatial probability density function whose form is that of a diffraction pattern, and if a telescope is considered which has a 4 inch aperture and is tracking a 2nd magnitude star, then the theoretical limit to pointing accuracy is about 10^{-3} seconds of arc (rms) for a one second integration time.¹⁴ Practical design problems prevent us from achieving this limit by a factor of at least two or three orders of magnitude for most star trackers. In contrast, the scanning camera which is described in the present paper will have a theoretical limit which is more nearly 1.0 second of arc for the same star and for a scan period of 10 seconds. An rms pointing accuracy of 10 seconds of arc places us within one order of magnitude of the theoretical limit. If we wish to measure the positions of significantly fainter stars, it will be necessary to extend the scan period or collect statistical data over a large number of rotations.

CHARACTERISTICS OF CELESTIAL TARGETS

The method of navigation described in the present paper requires the use of two kinds of targets. The stars which form one group are used to determine the attitude of the space vehicle. Solar-system bodies which form the other group are used to determine the position of the space vehicle once the attitude is known. Depending on the navigational accuracy needed, both groups will require the introduction of correction terms once a first estimate of the position and velocity is obtained. In the case of the stars correction terms for aberration will be required. In the case of the solar system bodies correction terms for planetary aberration, updating of the ephemeris and calculation of position of center of gravity from the limb measurements must be made.

Stellar Targets

Typically, the lower bias level for the photomultiplier will be set at about +2.0 magnitude, and targets which are fainter than this will not be recorded. With 60° scanning slits as shown in Figure 2 and with a camera field of view of 30° , we will detect stars within a region 26° wide (Figure 6). If the spin axis is normal to the ecliptic, approximately 10 stars will be available for attitude determination. These stars are shown in Table III. The positions of these stars in right ascension and declination¹⁵ have been converted to celestial latitude and longitude¹⁶ to show their relative positions along the ecliptic. The visual magnitude is shown in the last column. From Table III we can conclude that an ample number of stars near the ecliptic of sufficient brightness will be available for the attitude determination.

TABLE III: STARS LYING WITHIN $+13^\circ$ OF ECLIPTIC
WITH MAGNITUDES LESS THAN 2.0

General Cat. No.	Right Ascension			Declination			Celestial Lat. (Deg)	Celestial Long. (Deg)	Magnitude
	h	m	s	0	'	"			
5605	04	33	02.9	+16	24	37	-5.5	69.1	1.06
6681	05	23	07.8	+28	34	02	+5.3	81.9	1.78
8633	06	34	49.3	+16	26	37	-6.7	98.4	1.93
10120	07	31	24.7	+31	59	58	+10.1	109.5	1.58
10438	07	42	15.6	+28	08	55	+6.5	112.5	1.21
13926	10	05	42.7	+12	12	44	+0.4	149.2	1.34
18144	13	22	33.3	-10	54	04	-2.2	203.2	1.21
22157	16	26	20.2	-26	19	22	-4.3	249.1	1.22
25100	18	20	51.2	-34	24	37	-11.0	274.5	1.95
23769	17	30	12.6	-37	04	10	-13.7	263.9	1.71
25941	18	52	09.9	-29	21	39	-6.4	281.4	2.14
21489	15	57	22.3	-22	28	52	-2.1	242.0	2.54

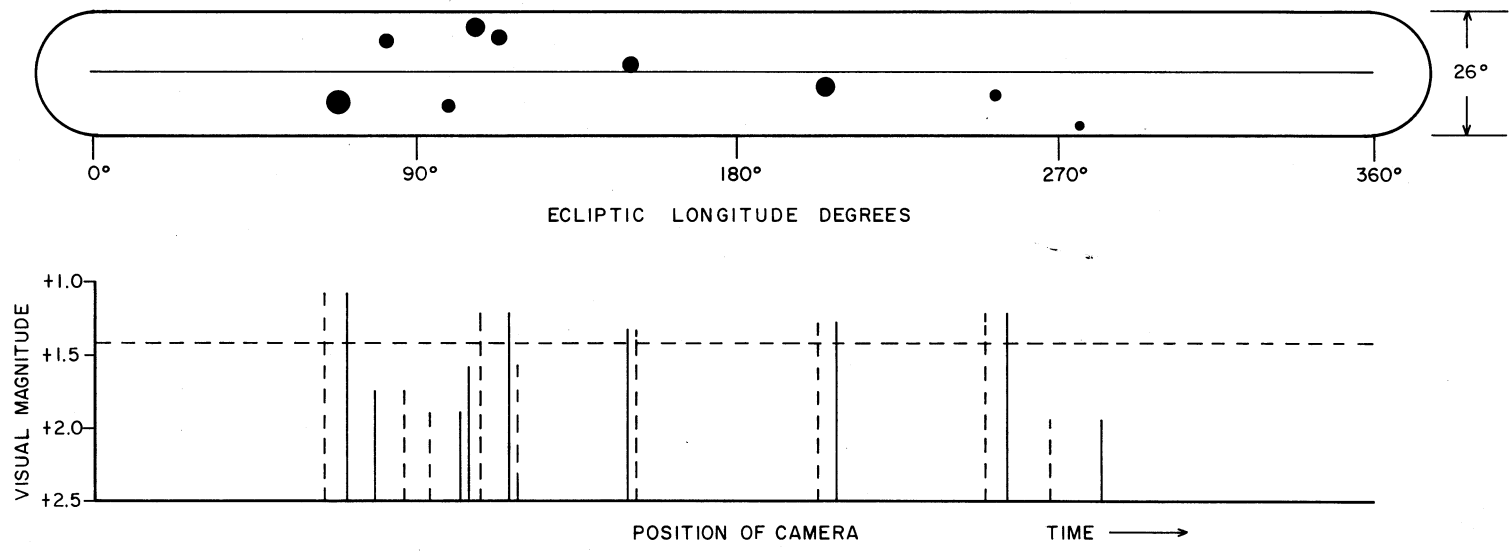
As the camera scans across the sky, the time of appearance and the brightness of the stars crossing the field of view will be recorded. An example of the star scan time pattern for the stars shown in Table III is shown in Figure 7. The order of the vertical solid and dotted lines indicates which photomultiplier was first actuated and therefore whether the star lies above or below the scan plane. The horizontal dotted line shows that only five stars will be recorded if the detection limit is set at a magnitude of 1.4. The specific set of stars above the detection limit depends on the spectral response of the photomultiplier. The data in Figure 7 apply only to the visual magnitude.

The background noise entering the slits from the large number of low intensity stars scattered throughout the sky will usually not be troublesome. However, occasionally an anomalous pulse form will be received because two bright stars enter a slit at the same time and these signals will be rejected by the computer. The probability of this occurrence increases with increasing slit width and therefore we are motivated to keep the slits as narrow as possible. The slits are 30° long and 1 minute wide, therefore the total area is 0.5 square degrees per slit. Taking the worst case for zero galactic longitude, the average number of stars per 0.5 square degree¹⁷ which are brighter than 4.5 magnitude (10% of the intensity of a 2nd magnitude star), is only 1.4×10^{-2} . This calculation establishes that on the average there will be very few strong signal events to interfere with the pulse time or intensity measurements. The question remains as to what background the average starlight from the entire sky contributes. It is equivalent to about 700 1st magnitude stars¹⁸ and it can therefore be shown that a single slit on the average will receive a background signal which is 2% of the intensity of a 2nd magnitude star. In certain regions near the galactic plane the background will be much larger than this, but even a background as large as 10% or 20% will not create a serious error in the scan time measurement.

Planetary Targets

In the case of the celestial bodies within the solar system, a somewhat different problem presents itself. In this case, we wish to determine the position of the limb of the body and therefore wish to know the apparent magnitude as a function of the angular emersion of the limb into the region of the slit. Figure 8 shows this relation for various normalized distances measured in astronomical units. Except for the dotted line for Mercury, the curves have been terminated when half of the planet has emerged into the slit. An approximation made in deriving these curves is that the intensity of the reflected light near the planetary limb follows Lambert's law.

Figure 7. Star Scan Pattern for Stars Near Ecliptic With Magnitude ≤ 2.0



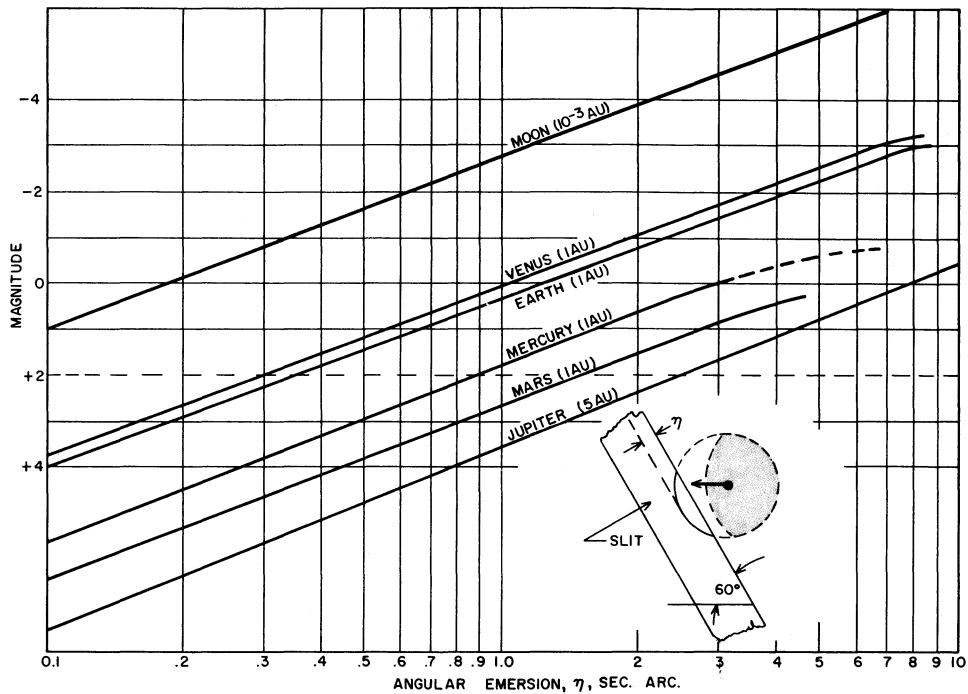


Figure 8. Planetary and Lunar Magnitudes at Various Angular Emersions

If we establish a lower bias level at +2 magnitude, all of the inner 4 planets will provide sufficient brightness at angular emersions less than 2 seconds of arc. In no case is this emersion greater than 20% of the diameter of the planet. As is shown with later calculations, if we approach the planets closer than the distances assumed in Figure 8, the extent of the angular emersion for a given magnitude will be further reduced. The optical system itself creates a blur circle of approximately 10 seconds of arc and thus the error introduced by the angular emersion required to provide sufficient brightness will usually be small compared with this value.

There are four solar-system bodies not shown in Figure 8 which can be detected by the camera on Mars or Venus trips. These are the Sun, Saturn, and the natural satellites of Mars-Phobos and Deimos. The Sun is too bright for the photomultiplier, although it might be detected by an auxiliary detector such as a silicon cell as was described previously. In certain cases the Sun would provide useful directional information for triangulation. Saturn has a maximum magnitude of about -0.2 at a distance of 9.5 AU and therefore has sufficient brightness for our detector. However, Saturn is so distant that the effect of a given angular position error will be about 10 times as great as for a planet

only 1 AU from the space vehicle. In addition, Saturn's rings complicate the problem introducing a correction term to find its center of gravity. At mean Martian opposition, the satellites Phobos and Deimos have visual magnitudes of +11.5 and +12.5 and are therefore not sufficiently bright to be useable for mid-course navigation. However, as a space vehicle approaches Mars, these satellites could provide useful information for terminal navigation.

Lunar Target

In addition to being useful for interplanetary navigation, the rotating wide angle camera can be used for navigation in cislunar space. In this case a simple triangulation using the Moon and the Earth would be used. As is shown in the Applications Section, the angular separation between the Earth and Moon is such as to permit accurate triangulation during most of the trip. With the reduced distances ($\approx 10^{-3}$ AU), the effect of the angle measurement error caused by the detection instrument is now of the same order of magnitude as the space vehicle position errors resulting from the errors in the definition of the position of the edges of the Moon and Earth. For example, at the midpoint, the range to the Earth or Moon is about 2×10^5 km. An instrument error of 5 seconds of arc therefore creates a position error of $2 \times 10^5 \times 25 \times 10^{-6} = 5$ km. By way of comparison, Figure 9 shows that the errors caused by the irregular shape of the edge of the Moon will average about 2 km. The contours in this figure are for various lunar latitudinal and longitudinal librations as seen from the Earth.¹⁹ Although they cover only a limited region of the lunar surface, they may be regarded as indicative of the height of lunar surface irregularities.

Since an emersion of 6 km results in a sector which is 300 km long, we might consider the possibility of improving the accuracy of the lunar limb measurement by averaging over an extended length. In this case we would require that the signal from the Moon be very large, say -4 magnitude, before we attempt to measure the position of the limb. It was found that this technique does in fact reduce the effect of isolated protuberances in the lunar profile; however, it was also found that the effect of variations in the albedo creates a much larger error when the emersion is large than when it is small.

The following derivation will show why this occurs. If the emersion is small, we may write according to the geometry of Figure 10, $\lambda = 2 \sqrt{D_m \cdot \eta}$, where D_m is the Moon's diameter. An integration of this equation yields for the area of the emerged segment

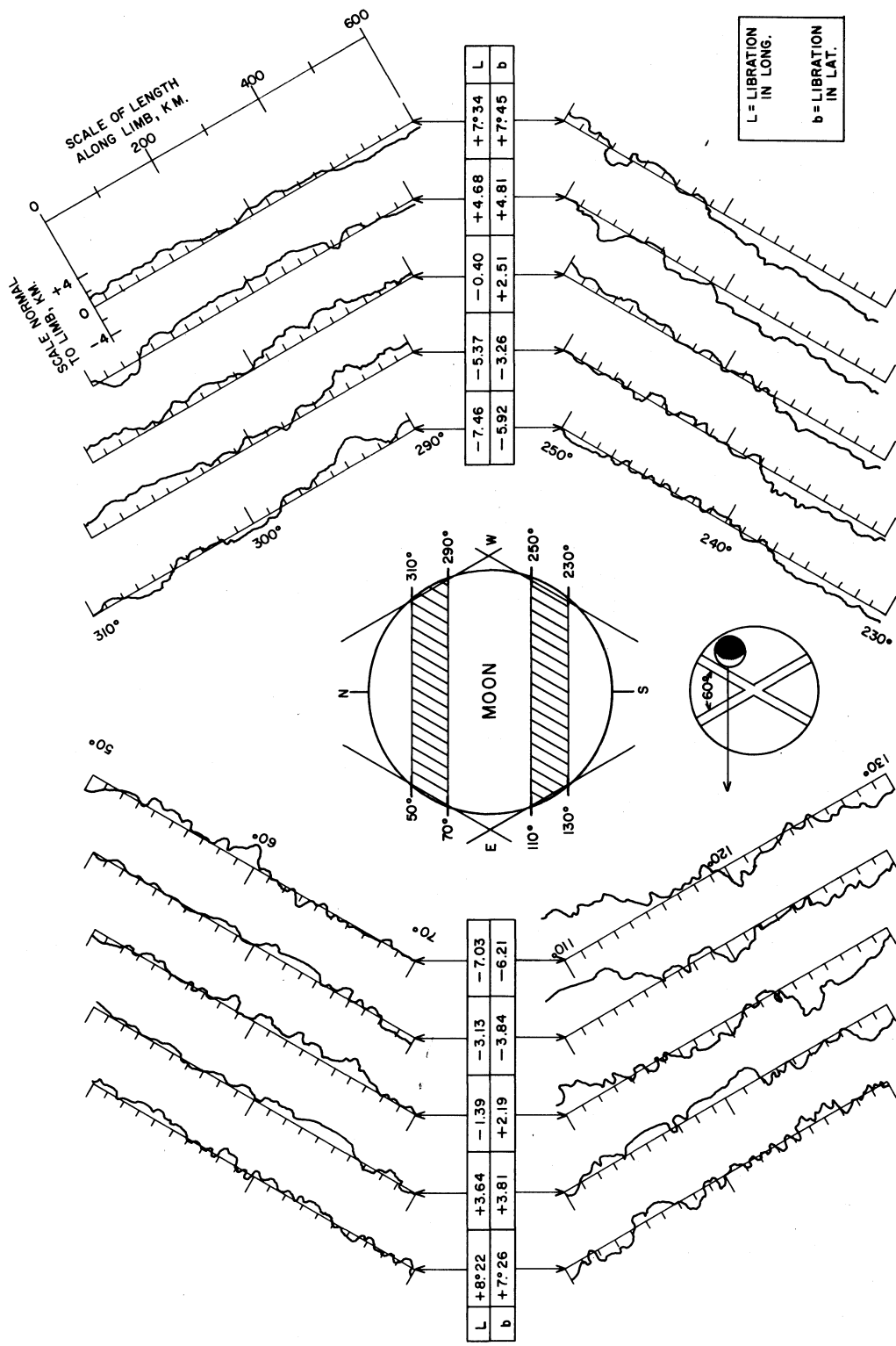


Figure 9. Contours of Lunar Limb for Various Librations

$$A_s = 4/3 D_m^{1/2} \cdot \eta^{3/2} \quad (2)$$

If we assume an average albedo across the emerged segment of α_1 , then the ratio of intensities of two segments is

$$\left(\frac{I_1}{I_2}\right) = \left(\frac{\alpha_1}{\alpha_2}\right) \cdot \left(\frac{\eta_1}{\eta_2}\right)^{3/2} \quad (3)$$

When the effect of varying solar incidence and reflection angles and the effect of varying albedos from the lunar maria to mountain ranges is considered²⁰, a small segment along the limb could have an albedo as small as 1/10 the average for the entire Moon. For this case if the emersion were η_1 for an average segment, it would have to increase to $\eta_2 = \eta_1 \cdot 10^{2/3}$ in order to produce an equivalent photomultiplier signal. If the average emersion is $\eta_1 = 6$ km, as was assumed above, this value would be increased to $\eta_2 = 28$ km, thus producing an error of 22 km. On the other hand, if the photomultiplier bias level were set so as to require an average emersion of only 1 km, the factor of 10 change in albedo would only cause the emersion to increase to 4.6 km - an error of 3.6 km.

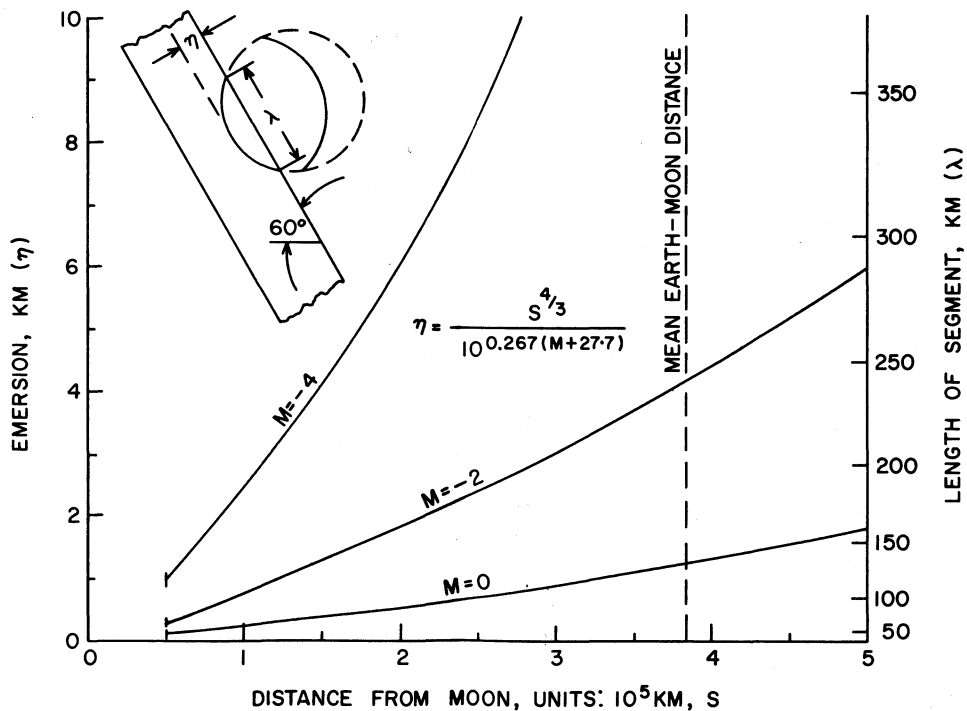


Figure 10. Lunar Emersion at Various Distances and Magnitudes (Moon Assumed to be Lambert Sphere)

Since the errors caused by the variation in albedo can be much larger than the errors due to poor averaging along the lunar limb, the most accurate limb position measurement will be obtained by using a low bias level, i. e., by minimizing the emersion and measuring the lunar transit time when the segment is equivalent to a magnitude of about 0.0. This means that we are not averaging the effect of lunar mountains, but this error will not exceed 4 or 5 km and will have an rms value less than 2 km.

The relation between the emersion, η , the distance of the Moon from the space vehicle, S , and the detection level measured in terms of magnitude, M , can be derived as follows. The magnitude of the Moon at a distance $S_1 = 3.84 \times 10^5$ km is $M_1 = -12.5$. The diameter of the Moon is $D_m = 3.48 \times 10^3$ km. Let I_t be the intensity of the radiation from the full Moon when viewed from a distance S_1 . Let the intensity of the radiation from the emerged segment of width, η , be I_s when viewed from a distance S . The ratio of the intensity of the radiation from the emerged segment divided by the intensity of the radiation from the full Moon is

$$\frac{I_s}{I_t} = \left(\frac{A_s}{A_t} \right) \left(\frac{S_1}{S} \right)^2 = \left(\frac{16}{3\pi} \right) \left(\frac{\eta}{D_m} \right)^{3/2} \left(\frac{S_1}{S} \right)^2 = 10^{0.4(M_1 - M)} \quad (4)$$

where we have used Equation (2) and the star magnitude - intensity relation. It is assumed that $\eta \ll D_m \ll S$. After substituting numerical values we may write

$$\eta = S^{4/3} \cdot 10^{-0.267(M + 27.7)} \quad (5)$$

where η and S are expressed in km. Figure 10 is a graph of this relation. For a constant bias level, M , as one approaches the Moon the emersion becomes progressively smaller.

The measurement of the position of the illuminated edge of the Earth presents a completely different problem because of the atmosphere. Typically, from the mid-course point on a lunar trip, the scattered radiation will be sufficient to reach +2 magnitude when the atmosphere above 80 km falls in the slit. This could be reduced to 40 km if the bias level were set at about -2 magnitude, and this would probably be advantageous. Generally we should avoid further increases in the bias level to such a point that the edge of the slit gets down to a level where cloud variability becomes a problem.

DETERMINATION OF POSITION

As shown in the introduction, the recommended method of position fixing is that of triangulation in which the stars are used for attitude determination and the planets for position fixing. This geometry was shown in Figure 4. In order that the detection instrument described in this paper be used for the determination of position in the solar system, its spin axis must be nearly normal to the ecliptic plane. Two planets provide a minimal basis for position determination and more than two planets provide a basis for the statistical determination of space vehicle position.

Triangulation

Consider the case in which two planets and the space vehicle are arranged as in Figure 11. The directions of the vectors \underline{R}_1 and \underline{R}_2 are the quantities measured by the sensor, while

$$\rho_1, \theta_1, \phi_1, \rho_2, \theta_2, \phi_2$$

are stored in the computer or computed from an ephemeris. Then:

$$\underline{\rho}_3 = \underline{\rho}_2 - \underline{R}_2 \quad (6)$$

$$\underline{\rho}_3 = \underline{\rho}_1 - \underline{R}_1 \quad (7)$$

These represent six equations for the solution of the five unknowns: $R_1, R_2, \theta_3, \phi_3, \rho_3$. R_1 and R_2 give the distances to the two planets in question, while ρ_3, θ_3 and ϕ_3 determine the position vector of the vehicle relative to the sun. From these, the distance to any other solar body may be computed as needed.

With regard to the general technique of position finding by triangulation, the geometry of the configuration imposes some restrictions. There are two sources of errors with this technique which must be minimized by proper selection of planets. One of these relates to the situation in which the two planets and the vehicle are collinear, and in which the position of the vehicle is undefined. The other relates to the length of the sight lines to the planets. For a given angular measurement error, the farther away the planet is, the greater is the resulting position error. One can visualize this as an "error cone" with apex at the planet and axis lying along the line from the planet to the space vehicle. The vertex angle of the cone is the same for each planet, but the size of the cone cross-section at the position of the vehicle is obviously a function of the planet-vehicle distance. Thus distant planets are also to be avoided.

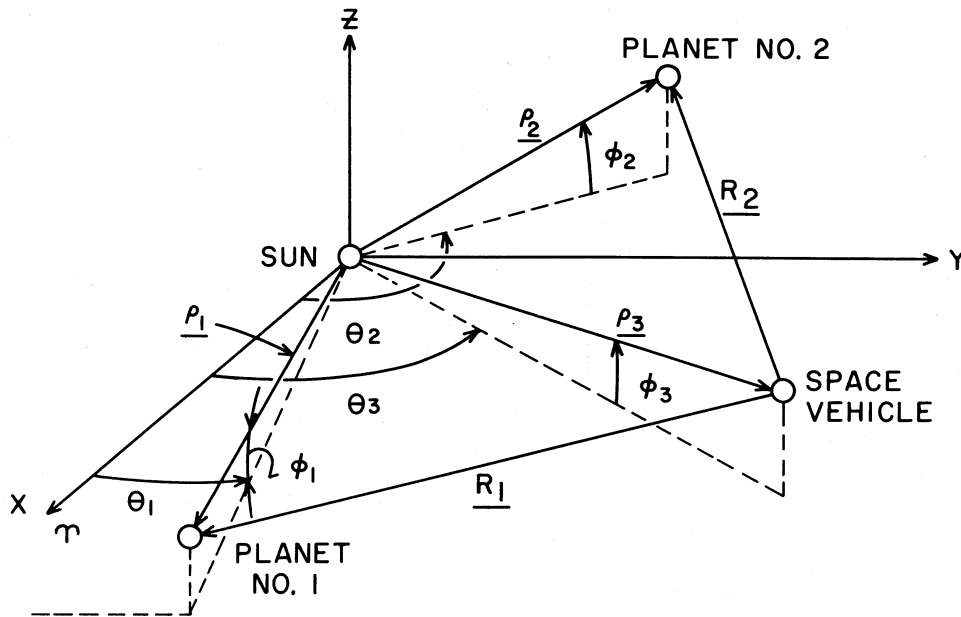


Figure 11. Geometry of Satellite Position Determination by Planetary Triangulation

Least Square Polyangulation

The navigational technique which involves the use of two-planet triangulation forms the basis for the present analysis. However, the nature of the observing instrument is that it scans the entire ecliptic and this means that more than two solar-system targets will be available for triangulation. Rather than perform a series of separate triangulations and then attempt to combine their results or to search for the best single triangulation, it was felt that a method was needed which statistically determined the position of the space vehicle.

The method which is derived below is similar to the well known Sumner Navigational Method which measures the zenith distance of several stars - each zenith distance providing a circle of position, and the intersection of two circles defining a point. The polyangulation method described in the present paper differs from the Sumner Method in the following respects.

- A. Each solar-system body defines a true "line of position" rather than a circle of position.
- B. The uncertainties associated with each solar-system line near the region of confluence differ grossly, while the errors of the various earth referenced zenith angle measurements are not greatly different.

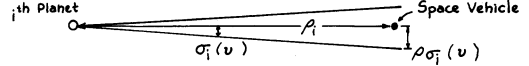
- C. Interplanetary navigation problem is three-dimensional; earth navigation is two-dimensional.
- D. The relative positions of the various solar-system bodies are continuously changing while the stars used in the Sumner Method require only minor positional corrections.
- E. In the earth navigation problem, the direction of the local gravity vector forms the reference for the angle measurement, while in the space navigation problem a stellar-inertial attitude reference is used.

The Saint Hilaire Method is a modification of Sumner's Method which also bears some resemblance to the space vehicle navigational problem in that this method measures the difference between the computed altitude for the desired position and the measured altitude. The altitude-difference tells the earth navigator the amount and direction of the correction in position. In most space navigation problems the desired trajectory will be known beforehand so that a computational simplification can be effected by calculating only differences in position²¹ as is done in the Saint Hilaire Method.

The space vehicle viewing geometry and the planetary position coordinates are shown in Figure 12. A heliocentric coordinate system is used in which the x-y plane coincides with the ecliptic. In order to simplify the drawing, only one planet is shown. The fact that the sight line does not intersect the space vehicle reflects the fact that an error will exist in the measurement of the direction of this sight line in inertial space. The normal line is defined as that line which passes through the space vehicle and which is orthogonal to the sight line. It is used to define the minimum deviation of the space vehicle from the sight line to the i^{th} planet, d_i .

The equations needed for the polyangulation technique are shown in Table IV. Equations (8) - (10) give the position of the i^{th} planet. The projection form of the equations of the sight line are given as Equations (11) and (12). The constants of these two equations are identified as Equations (13) and (16). These constants are established from the measured angular directions to the i^{th} planet, ν_i and ϕ_i , and the known position of the planet in ecliptic coordinates. Equations (17)-(19) define the coordinates of the space vehicle; Equations (20) and (21) establish the normal line. The

TABLE IV: EQUATIONS FOR POLYANGULATION

<p>POSITION OF i^{th} PLANET:</p> $x_i = P_i \cos \theta_i \cos \phi_i \quad (8)$ $y_i = P_i \sin \theta_i \cos \phi_i \quad (9)$ $z_i = P_i \sin \theta_i \quad (10)$	<p>INTERSECTION OF NORMAL LINE WITH SIGHT LINE:</p> $x_o = \frac{m_i (Y - b_i) + n_i (Z - c_i) + X}{1 + m_i^2 + n_i^2} \quad (22)$ $y_o = m_i x_o + b_i \quad (23)$ $z_o = n_i x_o + c_i \quad (24)$
<p>SIGHT LINE TO i^{th} PLANET AS SEEN FROM SPACE VEHICLE:</p> $y = m_i x + b_i \quad (11)$ $z = n_i x + c_i \quad (12)$ $m_i = \tan v_i \quad (13)$ $n_i = \frac{\tan \phi_i}{\cos v_i} \quad (14)$ $b_i = P_i \cos \phi_i [\sin \theta_i - \cos \theta_i \tan v_i] \quad (15)$ $c_i = P_i \left[\frac{\sin \theta_i \cos \phi_i - \cos \theta_i \cos \phi_i \tan \phi_i}{\cos v_i} \right] \quad (16)$	<p>SHORTEST DISTANCE FROM SPACE VEHICLE TO i^{th} PLANET SIGHT LINE:</p> $d_i^2 = [(x_o - X)^2 + (y_o - Y)^2 + (z_o - Z)^2] \quad (25)$ <p>WEIGHTED RESIDUAL DISTANCES FOR k PLANETS:</p> $R = \sum_{i=1}^k w_i d_i^2 \quad (26)$ <p>LEAST SQUARE EQUATIONS:</p> $\frac{\partial R}{\partial X} = \frac{\partial R}{\partial Y} = \frac{\partial R}{\partial Z} = 0 \quad (27), (28), (29)$
<p>POSITION OF SPACE VEHICLE:</p> $X = P \cos \theta \cos \phi \quad (17)$ $Y = P \sin \theta \cos \phi \quad (18)$ $Z = P \sin \theta \quad (19)$	<p>WEIGHTING FUNCTION FOR OBSERVATIONS OF i^{th} PLANET:</p> $W_i(v) = \frac{1}{\rho_i^2 \sigma_i^2(v)^2} \quad (30)$ $W_i(\phi) = \frac{1}{\rho_i^2 \sigma_i^2(\phi)^2} \quad (31)$
<p>NORMAL LINE FROM TRUE POSITION OF SPACE VEHICLE TO SIGHT LINE:</p> $y = M_i x + B_i \quad (20)$ $z = N_i x + C_i \quad (21)$	

parameters of the normal line need not be known, however Equations (22) - (24) yield the point of orthogonal intersection of the normal line and the sight line.

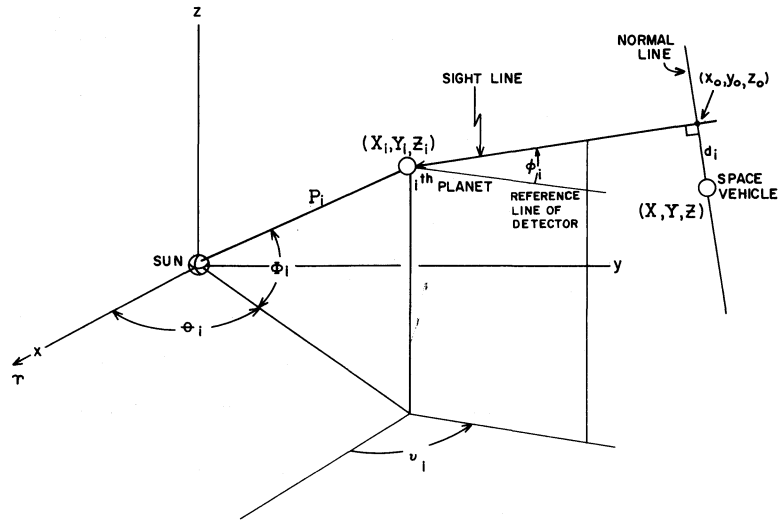


Figure 12. Polyangulation Geometry

It is now possible in Equation (25) to define the shortest distance of the space vehicle to the i^{th} planet sight line in terms of known quantities. These are the measured angular direction of the planet as seen from the space vehicle, the known position of the i^{th} planet, and an assumed but yet undefined position of the space vehicle. The calculated position of the space vehicle will be that position which minimizes the sum of the squares of the weighted residuals. Equations (27) - (29) provide three linear simultaneous equations in terms of X, Y and Z.

Equations (30) and (31) show what is probably the simplest form of the weighting function other than to assume it is a constant. In this case the weighting factor, $\rho_i \sigma_i(\nu)$, is proportional to the position uncertainty of the sight line at the estimated position of the space vehicle. ρ_i is the distance to the i^{th} planet and $\sigma_i(\nu)$ is the rms error in the angular position of the planet. As is necessary for minimized variance, the weights of the individual lines are inversely proportional to the variance of the position uncertainty. A variety of more complex weighting functions might be justified, but this is a problem which requires a detailed study of a particular detection instrument. Although the accuracy of the astronomical unit is likely to be improved considerably in the next few years²², it is not entirely valid to ignore the error in the absolute position of the various planets.

This is particularly true for values of $\sigma_i(\nu)$, $\sigma_i(\phi) \leq 10$ seconds of arc.

If the values of x_0 , y_0 and z_0 in Equations (22) - (24) are substituted in Equation (25), the Least Square Equations (27) - (29) can be evaluated. When this is done Equations (32) - (34) in Table V are obtained. A solution of these equations for the space vehicle position, X, Y and Z, yields the desired result.

The fact that more statistical data is available in the form of redundant angular measurements of planetary positions is not the main virtue of the least square polyangulation technique. The primary advantage lies in the fact that this method automatically weights the position determination in a manner which yields the least error sensitivity coefficients which can be obtained with a given set of data.

A different technique which involves the measurement of the angle between a star and a planet and which therefore leads to a "surface of position" has been described by Kleinhesselink and Christensen.²³ In order to simplify the analytical problem the approximate position of the vehicle is used, and the conoid representing the surface of position is replaced by a plane of position in a manner similar to that done in Earth surface navigation where tangent lines of position are used to approximate almucantar circles of position. The point of intersection of three planes of position defines the position of the vehicle; with more than three planes of position, a maximum likelihood estimator can be used to statistically define the position of the vehicle.

While a weighted least squares analyses may be performed with "planes, lines or points of position", the writers believe that the error pattern obtained with the instrument proposed in the present paper most logically leads to the use of a line of position. The errors in the angular position measurement of the stars will be smaller than the planets, and therefore the errors in establishing the orientation of the vehicle's coordinate frame can almost be disregarded as contributors to planetary angular position errors. In contrast, the use of surfaces of position, using one planet and one star, requires that we combine two measurements which have errors of different sizes. In addition, the nature of the proposed observing instrument is that certain of the systematic errors in the elevation angle measurement (ϕ in Figure 2) are cancelled, while both the random errors and

the systematic errors in the azimuth angle are present. Consequently the weight functions for azimuth and elevation angular measurements (Equations 30 and 31) will differ and the mathematical model should take account of this fact.

TABLE V: LEAST SQUARE POLYANGULATION EQUATIONS

$\sum_{i=1}^R W_i \alpha_i (m_i b_i + n_i c_i)$	$\sum_{i=1}^k W_i (\alpha_i - 1), \sum W_i \alpha_i m_i, \sum W_i \alpha_i n_i$		X	(34)	
$\sum W_i \{b_i - \alpha_i m_i (m_i b_i + n_i c_i)\}$	$-\sum W_i \alpha_i m_i, \sum W_i (1 - m_i^2 \alpha_i), -\sum W_i m_i n_i \alpha_i$	=	•	Y	(35)
$\sum W_i \{c_i - \alpha_i n_i (m_i b_i + n_i c_i)\}$	$-\sum W_i \alpha_i n_i, \sum W_i \alpha_i m_i n_i, \sum W_i (1 - n_i^2 \alpha_i)$		Z	(36)	

$$\alpha_i = \frac{1}{1 + m_i^2 + n_i^2}$$

APPLICATIONS

One of the most important characteristics of the type of instrument described in the present paper is its versatility. Thus, with the same optical instrument one can accomplish a multiplicity of tasks simply by providing a different computer program for each. Table VI summarizes these diverse methods of using the scanning camera and the present section will be devoted to the explanation of these techniques.

The capability of the system can be made completely self-contained, or if a communications link with the Earth is preferred, it can be used as a vehicle-borne sensor to feed data into an Earth-based computer. In the event one desires to use the instrument as a back-up navigational device for a manned vehicle, it is possible to effect a considerable simplification in the digital computer by allowing the operator to hand-calculate his position using previously prepared tables and charts.

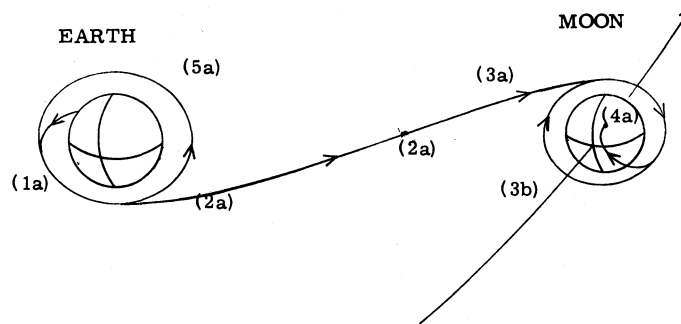
A possible sequence of operation for the tracker during a lunar landing mission is shown in Figure 13. In this case we have assumed that the initial orientation of the vehicle is completely unknown and that we are in an Earth-satellite orbit. After the establishment of an inertial reference, the detector would guide the vehicle to a rendezvous with a supply vehicle. Finally, after injection into lunar transfer orbit, the planet tracker may serve as a triangulator, determining the position of the space vehicle. In the event of a manned lunar probe, the camera can be used to orient the vehicle perpendicular to the Earth-vehicle-Moon plane. In this way, optimal conditions exist for viewing of the Earth and Moon through portholes in the vehicle. As shown in Figure 13, after the vehicle gets close to the Moon, the position determination can be more accurately performed by means of a different navigational mode. The direction to and apparent diameter of the Moon are measured. After the introduction of corrective thrusts sufficient to place the vehicle in a low altitude orbit around the Moon, the navigational mode could be changed again. In this case, it is assumed that a horizon scanner points the vehicle toward the Moon in the direction of the instantaneous local vertical. The planet tracker is pointed in a diametrically opposite direction to the horizon scanner. Finally, after landing on the surface of the Moon, the planet tracker is placed in a conical scan mode and the selenographic latitude and longitude are determined.

Attitude Determination

As shown in Table VI, there are two bases for attitude determination or for attitude control. The stellar-inertial method ties the orientation of the vehicle to two preselected stars and provides

TABLE VI: APPLICATIONS OF PROPOSED TRACKER

1. ATTITUDE DETERMINATION
 - a. Stellar-Inertial
 - b. Planetary
2. INTERPLANETARY NAVIGATION
 - a. Triangulation
 - b. Least Squares Polyangulation
3. SATELLITE NAVIGATION
 - a. Inertially Stabilized Vehicle
 - b. Radially Stabilized Vehicle
4. SURFACE NAVIGATION
 - a. Slowly Rotating Body
 - b. Rapidly Rotating Body
5. TRACK-WHILE-SCAN SEARCH
 - a. Rendezvous
 - b. Impact Avoidance



- (1a) Determination of inertial attitude while in Earth-satellite orbit.
- (5a) Rendezvous with additional supplies for lunar trip.
- (2a) Navigation by triangulation using Earth, Moon and 2 stars.
- (3a) Position determination by measurement of apparent diameter of Moon to obtain altitude and 2 stars for direction.
- (3b) Calculation of orbital elements for low altitude Moon-satellite orbit via vehicular radial stabilization.
- (4a) Determination of position of vehicle after landing on surface of Moon.

Figure 13. Sequence of Applications for Lunar Landing Mission

a means of monitoring the gyros for drift. The planetary method ties the orientation of the vehicle to two celestial bodies, say the Earth and the Moon, and the attitude of the vehicle is held constant in the Earth-vehicle-Moon plane.* The orientation within this plane is arbitrary and may be controlled by the operator so as to provide optimal viewing of the Earth, the Moon or in whatever direction desired. For a manned lunar vehicle this control is certainly desirable.

Interplanetary Navigation

In order to illustrate the use of the detection instrument for an interplanetary mission, an example was programmed on a Control Data 1604 Computer. This example involves a Hohmann transfer from Earth to Mars. This is a minimum energy transfer which has the shape of an ellipse.

In Figure 14 the positions of the Earth, Mars and the Vehicle are shown as a function of time. This figure is useful in studying the conditions for triangulation if one considers only the Earth, Mars and the Sun as possible target bodies. A more general presentation of the range and angle data is shown in Figure 15 and 16. Shown in dark lines are what appear to be the best targets for triangulation. However, as was described earlier, the position errors will be minimized if the least square polyangulation technique is used.

A program using a more realistic transfer is being processed at the present time. This grew out of discussions with R. W. Gillespie and uses criteria described by Breakwell, Gillespie and Ross.²⁴

* If the spin axis of the detector is normal to this plane, the time of transit of the edge of the Moon across the two slits is the same. If not, the difference in transit time will be approximately proportional to the deviation from the desired plane and can be used directly as a signal for attitude control.

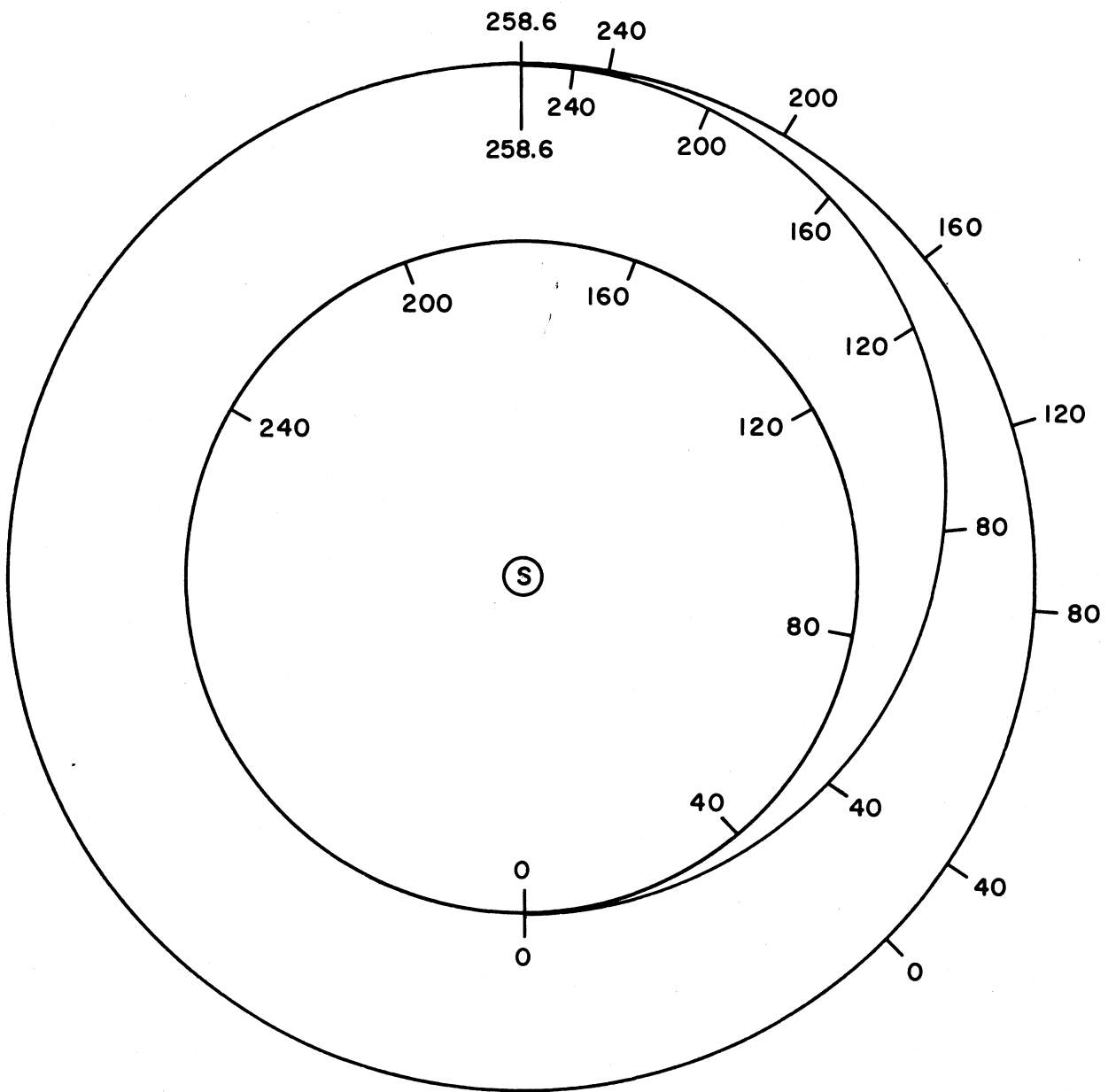


Figure 14. Positions (Days) of Earth, Mars and Vehicle for Hohmann Transfer

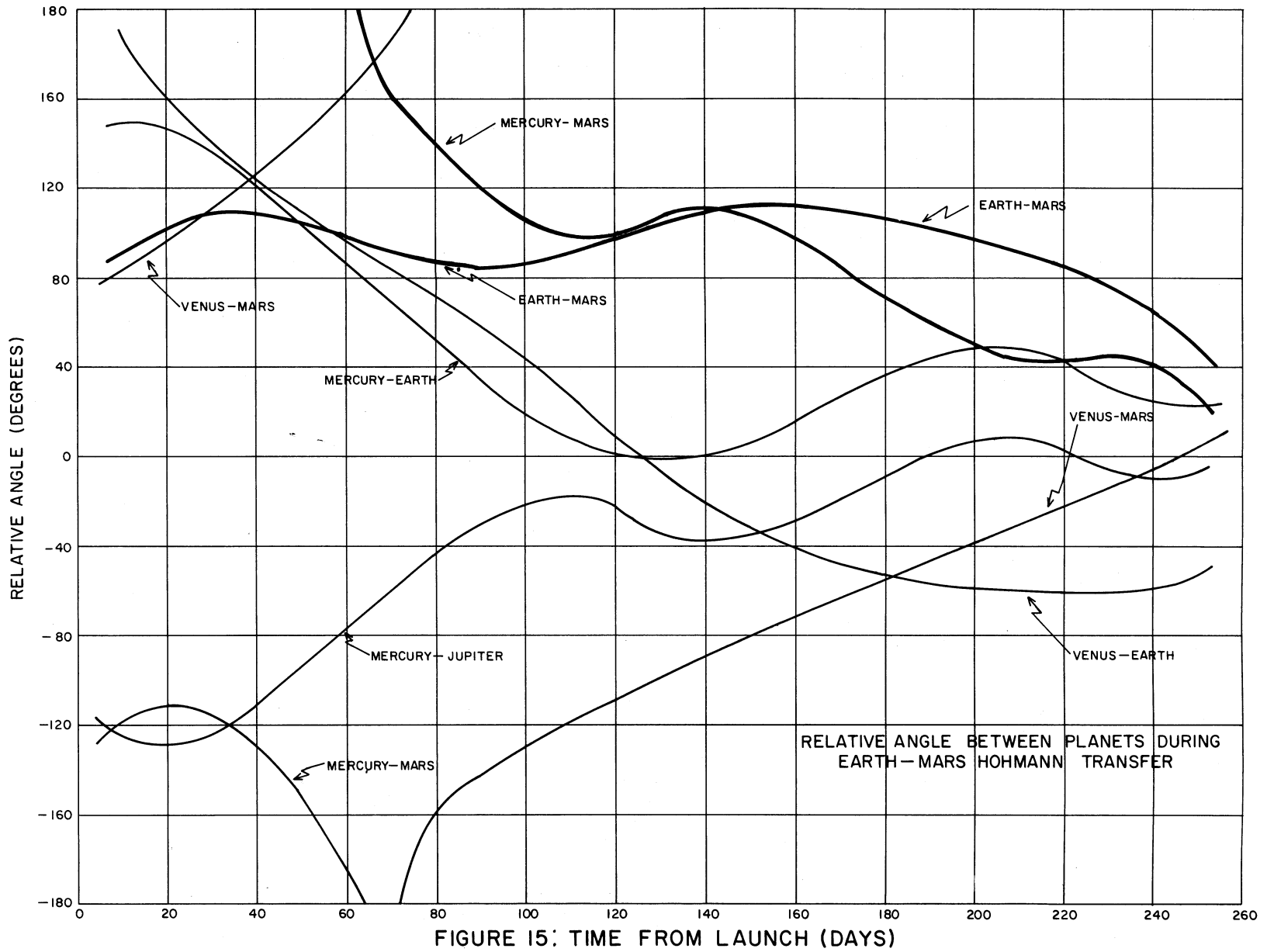


FIGURE 15: TIME FROM LAUNCH (DAYS)

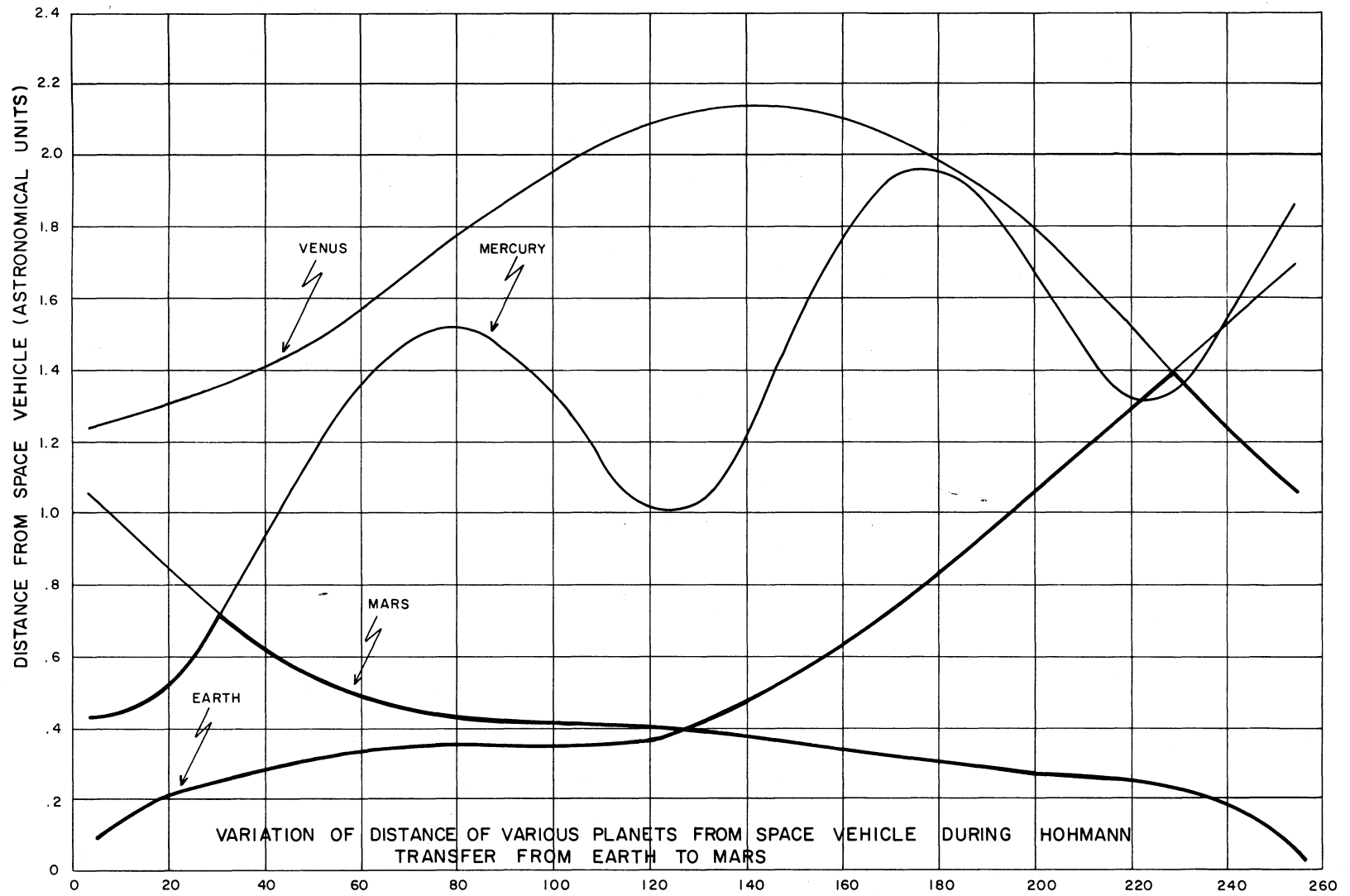


FIGURE 16: TIME FROM LAUNCH (DAYS)

Lunar Navigation

Since the detection instrument may also be used for navigation in cislunar space a number of circumlunar trajectories were studied. The effect of angle errors in the measurement of celestial bodies beyond the Earth-Moon system is excessively large because of their large distances, therefore a straight forward E-M triangulation is recommended. As before, the stars are used for establishing the attitude reference. However it is possible to regard other bright celestial bodies as sources of attitude information (not triangulation), if an ephemeris of the directions of these sight lines relative to the stellar coordinate frame for the particular transfer orbit in question is available.

The result of our study of the conditions for triangulation for circumlunar orbits is that accurate position fixing can be achieved during a large portion of the trajectory. Figure 17, published by Speer²⁵, illustrates one particular orbit. The angle between the Earth and the Moon as seen from the space vehicle is shown in Figure 18. The regions of poor triangulation where the relative angle is within $\pm 15^\circ$ of 0° or of 180° are crosshatched. It is to be noted that conditions are acceptable for triangulation during more than 90% of trip time to the Moon and return.

From the viewpoint of navigational accuracy one can consider two types of errors: (a) those errors arising from imperfections in the observing instrument, and (b) those errors inherent in the observational situation. Once the magnitudes of the errors inherent in the observational situation are determined, they will serve as a guide in establishing standards of accuracy for the observing instrument.

To be specific, consider the case illustrated in Figure 19. If the observing instrument makes an angular error in the measurement of the position of the lunar limb, then the effect of this angle error is proportional to the distance from the Moon and is given as $\delta \rho_e = \rho_m \cdot \delta \theta_m$. For the orthogonal intersection shown in this simplified example, the effect of this angle error is to cause an error in the calculated distance of the vehicle from the Earth.

On the other hand, because our observing instrument measures the position of the edge of the Earth or of the Moon, an error in our assumption regarding the position of this edge leads to a translational error in the position of the space vehicle as shown in Figure 19. For the instrument described in the present paper, we must contend with irregularities in the shape of the edge of the

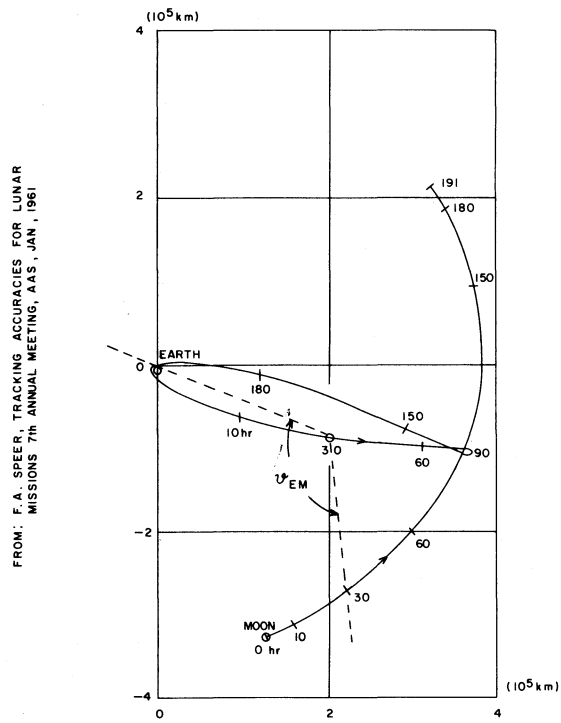


Figure 17. Circumlunar Orbit

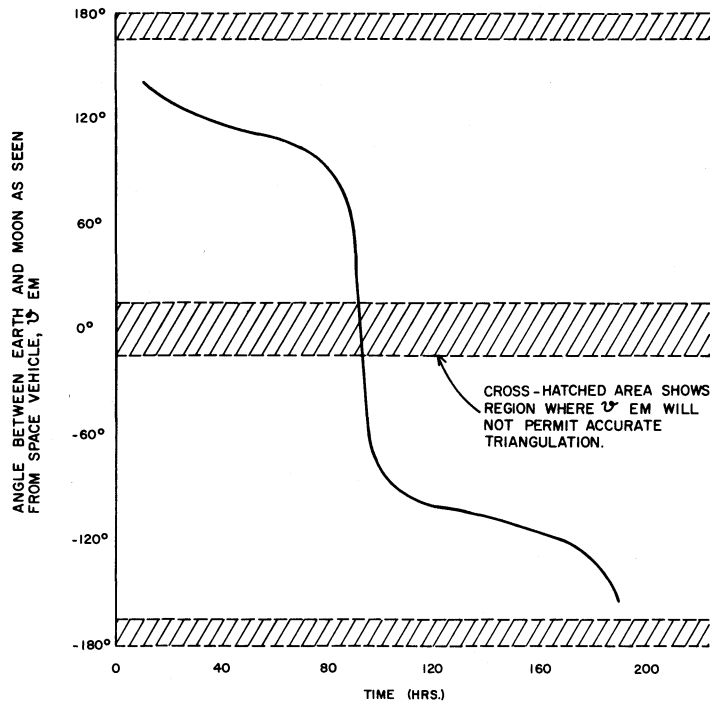


Figure 18. Earth-Moon Angle as a Function of Time During Circumlunar Orbit

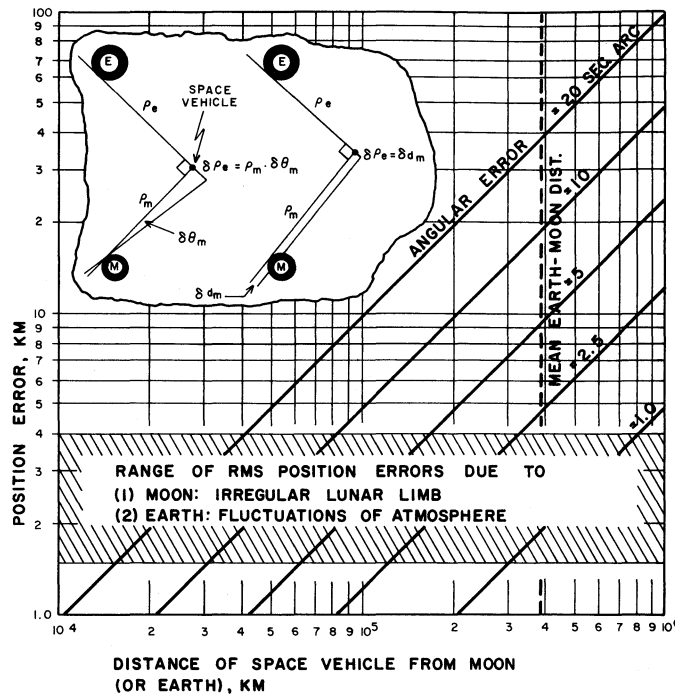


Figure 19. Comparison of Effect of Instrument Angle Errors in Calculation of Position of Space Vehicle

Moon and with variations in the reflectivity of the lunar surface. The more accurately these quantities are known the smaller will be δd_m in Figure 19. This is also true in defining the position of the edge of the Earth, and because of the Earth's atmosphere one must introduce various corrective factors to define the altitude at which a given amount of solar radiation will be scattered in the direction of the detection instrument.

A study of the problem of defining the position of the edge of the Earth and the Moon has been conducted and an rms position error of the order of 1. to 5 km will be found in defining the position of the edges of the Earth and Moon. The size of this error depends to a considerable extent on the complexity of the correction functions one uses in defining the limb position. The curves on Figure 19 show a comparison of the effects of translational errors in defining the position of the limb of the Earth or Moon with the instrument angular errors.

For example, if we were to make an angular error of 2.5 seconds of arc and if this error were made when the space vehicle is at a distance of roughly 1/2 the Earth-Moon distance, then an error

of about 2.5 km in the position of the space vehicle will result. This is about the same size as the translational errors resulting from limb uncertainties. From Figure 19 we may therefore conclude that the observing situation in cislunar navigation justifies a planet tracker with an accuracy of the order of 2 to 5 seconds of arc. An angle accuracy of 5 seconds of arc is within the potential of the planet tracker described in the present proposal and it appears that it can achieve an rms positional error of the order of 10 km in a self-contained manner.

Satellite Navigation

When the vehicle is close to the Moon, the Earth, or some other planet, the planet tracker can be used in two other ways (than triangulation) for navigation. These methods are summarized in Figure 20.

The method shown in Figure 20A involves the same operating mode as is used for triangulation except that a third slit is used to enable one to calculate the apparent angular diameter of the planet.

This is found from

$$\sin(M\omega + \rho) = \frac{\sin \rho}{\sqrt{1 - \sin^2 \alpha/2 \cos^2 \phi}}$$

where

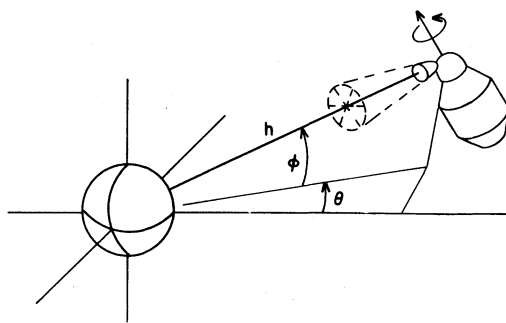
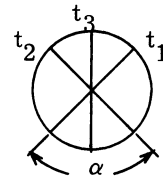
2ρ = apparent angular diameter of planet

α = angle between slits

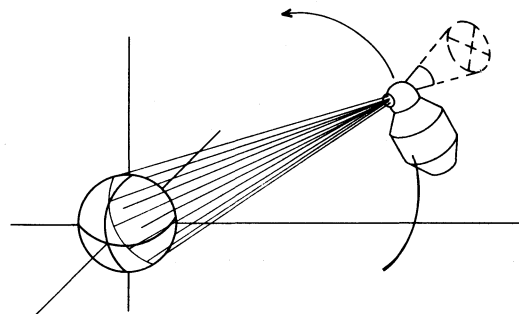
ω = spin rate

ϕ = elevation angle of center of planet as it passes across camera FOV

$$M = t_3 - \left(\frac{t_1 + t_2}{2} \right)$$



A. 3 SLIT METHOD ENABLES US TO MEASURE ANGULAR DIAMETER OF PLANET. STARS PROVIDE REFERENCE DIRECTION TO PLANET.



B. HORIZON SCANNER POINTS TOWARD LOCAL VERTICAL. TRACKER POINTS IN OPPOSITE DIRECTION AND MEASURES STELLAR SLIT SCAN TIMES.

Figure 20. Methods of Satellite Navigation

Knowledge of the diameter suffices to determine the space vehicle distance from and direction to the planet after star reference data gives the necessary attitude. This method cannot be used at altitudes less than 1.44 planetary radii as is shown below. At altitudes greater than about 10 planetary radii the three-slit geometry introduces errors which are greater than those resulting from two-body triangulation. Hence, the third slit is useful over a limited range of altitudes or when the space vehicle is in the neighborhood of a planet.

The Three-Slit Method, or for that matter the Two-Slit Triangulation Method, breaks down after the space vehicle comes within a certain minimum distance from the planet. This occurs because the apparent image of the planet no longer can be made geometrically tangent to the two crossed slits. The minimum altitude may be written

$$h_m = R \left\{ \sqrt{\left(\frac{\tan \alpha/2}{\sin b/2}\right)^2 + 1} - 1 \right\} \quad (35)$$

where the quantities in Equation (35) are as defined in Figure 21. The dotted lines show that for the recommended optical design a minimum altitude of about 1.44 planetary radii can be achieved. The minimum altitude increases relatively rapidly as we cut down the field of view of the camera or as we increase the angle between the slits. Probably the lowest altitude one can hope to achieve with a high quality optical system (FOV = 50°; slit angle = 30°) is about .18 R. For the Earth this implies a minimum altitude of 700 miles and the Moon 200 miles.

The method shown in Figure 20B involves essentially a different operating mode than does the triangulation technique or the direction-altitude technique and the minimum altitude considerations of Figure 21 do not apply to this method. In this case it is assumed that an infrared horizon scanner continuously points the space vehicle at the planet center or more precisely radially inward. This is a natural operating mode when the space vehicle orbits about any celestial body and is frequently used on Earth satellites. The planet tracker is pointed opposite to the horizon scanner and measures the time of appearance of a minimum of three stars. From this data the orbital elements can be derived; from the orbital elements, the position of the space vehicle as a function of time can be calculated. Equations for this method of position determination have been derived. This technique will work at any altitude where the vehicle orbit will maintain a reasonable amount of stability and at which the horizon scanner will return a continuous planetocentric orientation.

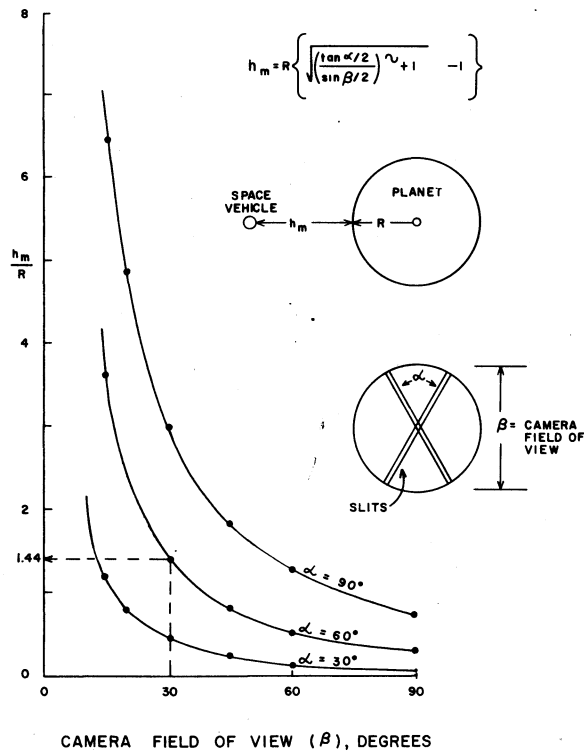


Figure 21. Minimum Operational Altitude for Triangulation

Surface Navigation

There are several ways in which the proposed instrument can be used after landing on the surface of a celestial body. For purposes of discussion these techniques are considered in two parts: (a) for a vehicle which has made contact with a slowly rotating body such as the Moon and (b) for a vehicle resting on a rapidly rotating or tumbling body such as one of the minor planets.

If the tracker is pendulously supported so that its rotational axis is parallel with the local vertical at some point on the Moon, it is possible to calculate the astronomic latitude and longitude of the observing station, as before, by measuring the slit scan times associated with at least two stars. Typically the optical axis is inclined upward at an angle of about 30° . This would be done to keep the scan region above the local terrain irregularities and it results in a conical scan path. The absolute elevation angle need not be accurately known during this operation, however it is important that the scan axis be accurately aligned relative to the local vertical. If the leveling errors can be kept small compared with the star transit time errors, an astronomic position measurement on the surface of the Moon accurate to better than 100 meters could be achieved.

A correction must be introduced because the rotational motion of the Moon changes the position of the stars during the period of one rotation of the camera, however, this correction is small for a body rotating as slowly as the Moon.

If the space vehicle were to land on a small and rapidly rotating body, and if the orientation of the detector were fixed relative to the body, then the measurement of star transit times would suffice for the determination of the direction of the spin axis of the body in inertial space. The precessional or nutational motions of the celestial body could be studied also. This problem is in many respects similar to the problem of the spinning space vehicle discussed earlier. On the other hand, if the body had a sufficiently strong gravitational field one could pendulously suspend the camera so that the optical axis pointed out into the sky in a direction diametrically opposite to the gravity vector. In this case the latitude of the vehicle relative to the planetary angular momentum vector could be calculated.

Track-While-Scan Search

Thus far emphasis has been placed upon the use of the proposed instrument to measure the angular bearing of a limited number of targets whose positions are changing relatively slowly. In addition to these applications, the proposed instrument can be used to keep track of a multiplicity of targets which are distributed over a broad region of the sky and whose positions are rapidly changing. In fact, it is exactly in this type of operation that the proposed instrument finds its greatest advantage over a typical tracking theodolite with its narrow field of view and its inability to handle more than one target at a time.

If the camera were supplied with an elevation axis gimbal so that it could be used in a conical scan mode, it can perform a useful role in rendezvous with other satellites and space vehicles. One assumes that the satellite on which the detector is mounted orients itself toward the sub-satellite point so that the scan region can be kept above the horizon.

If a vehicle were to pass through the asteroid belt on the way to Jupiter, the problem of impact avoidance might present itself. In addition, measurements of the relative abundance and motion of nearby asteroids would have scientific interest. Figure 22 shows the maximum asteroidal diameter visible from various ranges, assuming an albedo of 0.06. In deriving this figure it was also assumed that the solar aspect angle is such as to yield a 50% illumination.

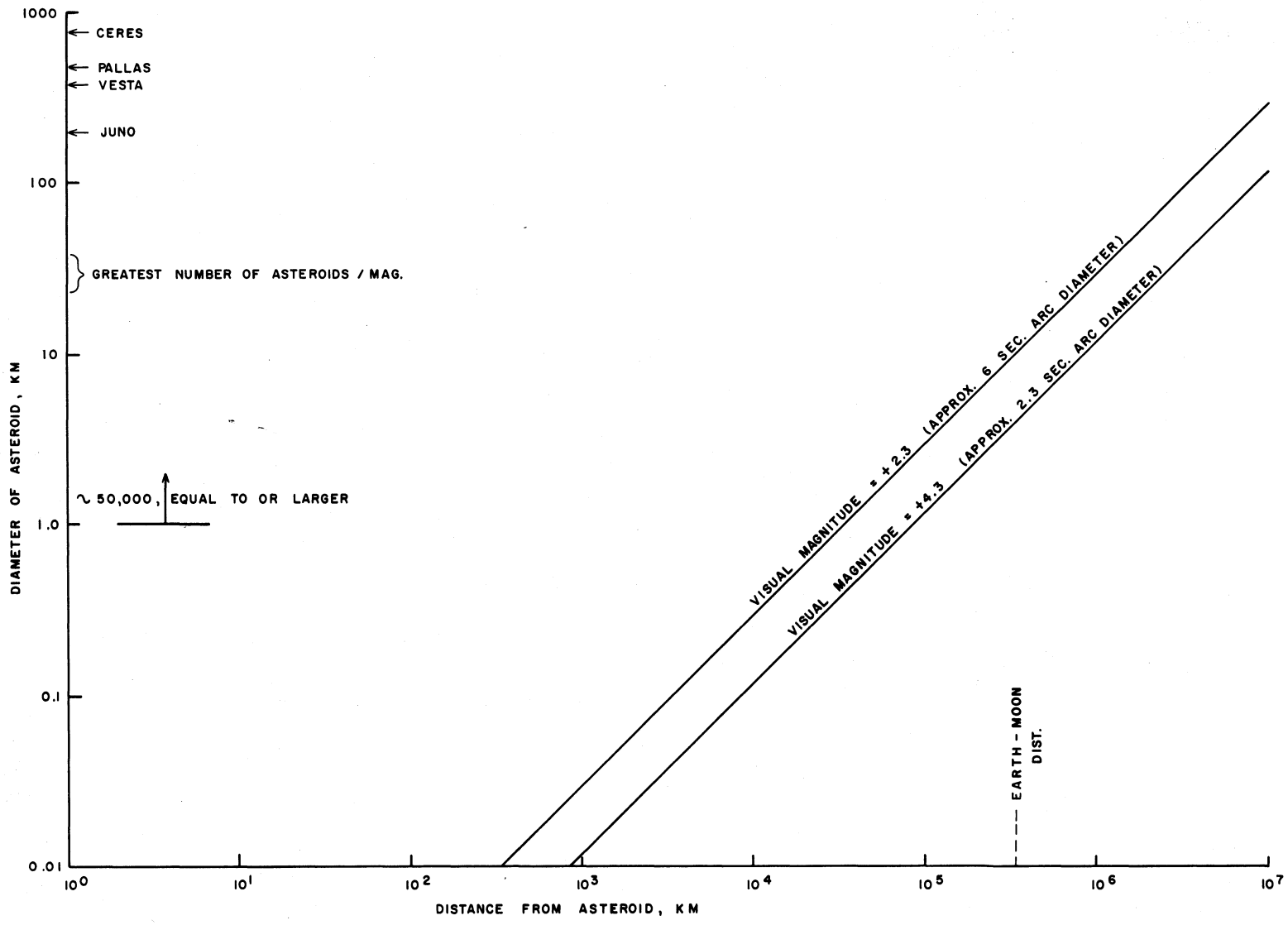
If the lower bias limit were set at +2.3 magnitude, it would be possible to see an asteroid of 100 meters diameter from a range of about 3×10^3 km. Typically an asteroid might be rotating around the Sun with a velocity of 15 km/sec. If one assumes that this is the relative velocity of approach of an asteroid and the space vehicle, then an asteroid of 100 meters diameter which is on a collision course will be visible to the instrument 200 seconds before impact. Larger asteroids could be detected earlier.

The diameter, albedo and average visual magnitude of the several of the larger asteroids are given in Table VII. These can be seen at considerable distances even with a lower bias level of +2.3 magnitudes. For example, Vesta can be seen from a distance of about 0.15 AU or 2.2×10^7 km. Characteristically the asteroids have rather large orbital inclinations as can be seen by the data in Table VII. A mean value is given as $\bar{i} = 9^\circ.7$ by Watson²³ and this probably would have some effect on the camera design. The presently proposed field of view of 30° permits the scanning of a region which is $\pm 13^\circ$ on either side of the ecliptic; however, an enlargement of the field of view to 50° would lead to a scan capability of $\pm 22^\circ$ on either side of the ecliptic.

TABLE VII: ASTEROIDS

NAME	DIAMETER (KM)	ALBEDO	AVG. VIS. MAG. (OPPOSITION)	SIDEREAL PERIOD (DAYS)	a (AU)	e	i (DEGREES)
Ceres	740	0.06	6.6	1681	2.767	0.079	10.6
Pallas	480	0.07	7.2	1684	2.767	0.235	34.8
Juno	200	0.12	8.2	1594	2.670	0.256	13.0
Vesta	380	0.26	5.8	1325	2.361	0.088	7.1

Figure 22. Maximum Diameter Asteroids Visible from Various Ranges
 (50% Solar Illumination) (Albedo = 0.06)



ACKNOWLEDGEMENTS

The project from which the material for the present paper was drawn has been sponsored by the Research Division of the Control Data Corporation under the direction of W. R. Keye.

The authors are particularly indebted to Rollin W. Gillespie of the Lockheed Missiles and Space Division for his suggestions regarding the selection of the interplanetary orbits used in the Applications Section.

We wish to thank Sandra Pippitt, Irwin Weisman and others for their assistance in preparing the manuscripts.

REFERENCES

1. Larmore, L., "Celestial Observations for Space Navigation", Aero/Space Engineering, January 1959, pp. 37-42.
2. Bement, H. D., "Stellar-Inertial System Looks Best for Interplanetary Mid-course Guidance", Space/Aeronautics, May 1961, pp. 128-132.
3. Bock, C. D., "A High Precision Stellar Navigator for Interplanetary Guidance", IVth Symposium on Ballistic Missiles and Space Technology, August 24-27, 1959, UCLA, Los Angeles.
4. Cardozo, A. L., "Automation for Interplanetary Navigation", IXth International Astronautical Congress, 1958, p. 652.
5. de Kler, J. J., "On the Degree of Accuracy to be Attained by Astro-Scanners as an Aid in Automatic Interplanetary Course-Computation", IXth International Astronautical Congress, 1958, p. 669.
6. Willmore, A. P., "A New Method of Tracking Artificial Earth Satellites", Nature, 182, 1008 (1958).
7. Groves, G. V. and Davies, M. J., "Methods of Analyzing Observations on Satellites", Xth Annual International Astronautical Congress - II, 1958, pp. 933-946.
8. Carroll, J., "Interplanetary Navigation by Optical Resection and Inertial Systems", Aero/Space Engineering, March 1959, p. 53.

9. Atkinson, R. d'E., "Some Problems of Interplanetary Navigation", Jour. Inst. of Navigation, Vol. 3, No. 4, 1950, pp. 365-377.
10. Stearns, E. V., and Frye, W. E., "Interplanetary Navigation: An Extension of an Ancient Art", Jour. Inst. of Navigation, Vol. 6, No. 8 (Winter 1959-60), pp. 526-535.
11. Newkirk, H. L., Haseltine, W. R., and Pratt, A. V., "Stability of Rotating Space Vehicles", Proceedings of the IRE, April 1960, pp. 743-750.
12. Goldstein, H., Classical Mechanics, Addison-Wesley, Reading, Mass., 1959.
13. Henize, K. G., Advances in Space Science, Vol. 2, Ed. by F. I. Ordway III, "Tracking Artificial Satellites and Space Vehicles", Academic Press, N. Y., 1960.
14. Lillestrand, R. L., Advances in Astronautical Sciences, "Test of Theory of Relativity by Measurement of Gravitational Light Deflection", Vol. 6, Macmillan Co., N. Y., 1961, pp. 871-898.
15. Becvar, A., Atlas Coeli, Skalnaté Pleso II, Epoch: 1950, Prague.
16. Tillitt, H. E., Astronomical-Coordinate-Conversion Table, U.S. Nav. Ord. Test Station, China Lake, Calif., 1958.
17. Forsythe, W. E., Smithsonian Physical Tables, IXth Revised Edition, Pub. by the Smithsonian Institution, Washington, D. C., 1954, p. 756.
18. Ibid., p. 757.
19. Weimer, T., Atlas de Profils Lunaires, Observatoire de Paris, 1951.
20. Bennett, A. L., "A Photovisual Investigation of the Brightness of 59 Areas on the Moon", Astrophysical Jour., Vol. 88, No. 1, 1938.
21. Baker, R. M. L., "Note on Interplanetary Navigation", Jet Propulsion, Dec. 1958, p. 834.
22. McGuire, J. B., Spangler, E. R. and Wong, L., "The Size of the Solar System", Scientific American, April 1961, pp. 64-72.
23. Kleinhesselink, G. J., and Christensen, R. R., "A Technique for Mid-course Interplanetary Navigation", XVIIth Annual Meeting of the Institute of Navigation, June 1961, Williamsburg, Virginia.

24. Breakwell, J. V., Gillespie, R. W., Ross, S., "Researches in Interplanetary Transfer, "
American Rocket Society Journal, February 1961, pp. 201-208.
25. Speer, F. A., "Tracking Accuracies for Lunar Missions", XIIth Annual Meeting of the American
Astronautical Society, Dallas, Texas, January 1961.